UNIVERSITY OF NAIROBI

STANNIC RUTILE TETRAGONAL TIN OXIDE GROUND STATE AND OPTICAL PROPERTIES STUDIED BY LOCAL SPIN DENSITY APPROXIMATION, THE GREENS FUNCTION AND BETHE SALPETER EQUATION.

BY

JOHN W. MASIKA

I56/69040/2013

A PROJECT SUBMITTED IN PARTIAL FULFILMENT OF THE REQUIREMENTS FOR THE DEGREE OF MASTERS OF SCIENCE IN PHYSICS OF THE UNIVERSITY OF NAIROBI.

April, 2015

DECLARATION

DECLARATION BY THE STUDENT

I declare that this project is my original work that has not been presented in any other university. No part of this project may be reproduced without prior written permission of the author and University Of Nairobi.

SIGNATURE:..... .....DATE.....

NAME: MASIKA W JOHN
REG. NO.: I56/69040/2013

DECLARATION BY THE SUPERVISORS.

This project has been submitted for examination with our approval as University Of Nairobi supervisors.

SIGNATURE:..... DATE:.....

NAME: Dr. Robinson Musembi
Department of Physics , University of Nairobi

SIGNATURE:..... DATE:.....

NAME: Dr. David Wamalwa.
Department of Physics, University of Nairobi

SIGNATURE:..... DATE:.....

NAME: Prof. Julius Mwabora
Department of Physics, University of Nairobi

DEDICATION.

I dedicate this work to my family and all physicists interested in computation physics.

ABSTRACT

Tin occurs in two main oxides; stannic oxide (SnO 2) and stannous oxide (SnO). The two oxides depicts the dual valence of tin, with oxidation states of 2+ and 4+. Stannous oxide is less well characterized than SnO_2. Its electronic band gap is not accurately known but has been estimated to be somewhere in the range of 2.5–3 eV. Thus stannous oxide exhibits a smaller band gap than stannic oxide, which is largely quoted to be 3.6 eV. There are no single crystals available that would facilitate more detailed studies of stannous oxide. As such not much has been done about this oxide. Stannic oxide is the most abundant form of tin oxide [10] and it has more technological significance in gas sensing applications, photo electronic applications and oxidation catalysts. Furthermore besides its common rutile tetragonal structured SnO2 phase there also exists a slightly more dense orthorhombic high pressure phase. Suito et al. showed that in a pressure–temperature diagram the regions of tetragonal and orthorhombic phases can be separated by a straight line of the equation p (kbar) = 140.0 + 0.022T (°C).

Owing to the vast applications of stannic Tin Oxide in the field of transparent conducting metal oxides, this project seeks to establish the structural properties, electronic and optical properties of stannic rutile tetragonal tin oxide using purely theoretical predictions. In this project, the ground properties of SnO2 have been studied using Quantum-ESPRESSO code, while the optical properties have been probed using *yambo code*. The ground state properties are studying using the Local Spin Density Approximation (LSDA). The band gap of SnO2 is found to be 3.6eV a value that agrees with the theoretical value. The Greens Function and the dynamically screened interaction (GW) and the Bethe Salpeter Equation (BSE) have been used to study the absorption energy and the electron energy loss spectra. By the BSE, the value of the band gap is found to be 3.5eV which is close to the available experimental values showing a variance of -2.78% from the experimental value. The absorption spectra obtained from the BSE calculations show that the maximum light absorbed by SnO2 is in the UV wavelength near 10nm which posses that SnO2 is a good absorber of UV of the electromagnetic spectrum. The following SnO2 parameters were used in this work: a=b= 4.1485A° and c=2.6620A°[1,3,6] . This was done by computational methods on SnO2 under its normal manifestation.

ACKNOWLEDGEMENT.

I thank the UNIVERSITY OF NAIROBI and more so the Department of Physics together with the Computational Materials Science Group, Department of Physics UNIVERSITY OF ELDORET for allowing me to use their facilities for my research. I would like to appreciate my supervisors Dr. Musembi and Dr Wamalwa for their constant support throughout my research. I would also like to appreciate Prof. Amollo and Dr. Makau for facilitating my stay at University of Eldoret and constantly giving direction during my research. I thank Mr. Felix for his undying support throughout my research period. Thank you very much for your assistance. I extend my acknowledgments to the University of Eldoret community for enabling me to do my work and my friend Gilbert for accommodating me during the research period. In a special way I than my family for trusting me and being with me through all my work financial, morally and socially. Its my pleasure to appreciate my colleague Isaac Obegi who we have shared this experience and worked together like brothers at all times.

GLOSSARY

SnO	Stannous tin oxide
SnO2	Stannic tin oxide
bc	Body centered
LSDA	Local Spin Density Approximation
DFT	Density function theory
GW	Greens function and dynamically screened interaction
BSE	Bethe Salpeter Equation
RPA	Random Phase Approximation
LDA	Local density approximation
ESPRESSO	opEns Source Packages for Research in Electronic Structure, Simulations and Optimization.
GGA	General Gradient Approximation.
DOS	Density Of States.
PDOS	Projected Density Of States
eV	Electron Volts
TCO	Transparent Conducting Oxides
UV	Ultraviolet
scf	Self-consistent wave-functions
nscf	Non-self consistent wave-functions
ks	Kohn-Sham
BZ	Brillouin zone

Contents

CHAPTER ONE.

1.0 INTRODUCTION.

1.1 Rutile Tetragonal Stannic Tin Oxide (SnO_2)

Tin oxide is the simplest of the transparent conducting oxides (TCOs) with an n-type band structure. This project focused on the rutile tetragonal structured SnO_2 which closely resembles the structure of TiO_2[1]. It has the rutile structure, in which each tin atom is surrounded by six oxygens in an octahedral array, and each oxygen is surrounded by three tin atoms in a planar array[1,3]. Its lattice calculated parameters are a=b= 4.1485A° and c=2.6620A° [1,3,6]

Tin is element 50 in the periodic table whose electronic configuration is 1s2 2s2 2p6 3s2 3p6 4s2 3d10 4p6 5s2 4d10 5p2/ [Kr] 5s2 4d10 5p2 per shell: 2,8,18,18,4 with a mass of 118.71 u[7]. Being a diamagnetic [12] TCOs, tin oxide is heavily used for flat panel displays, photo voltaic cells, low emissivity windows, electro chromic devices, sensors and transparent electronics[4,8,9,11]. Previous works on SnO_2 predict this structure to having both a direct and in-direct band gap of 3.6eV in different phases[4,8].

1.2 Ab Initio studies.

Theoretical methods and computational physics technology has gone through tremendous changes in the recent past. This has created a new platform for the researchers to research on material properties from first principles. This has made it possible for the researchers to be able to study ground state properties of materials for complicated systems which have strong many-electron interaction effects. Theoretically determining the properties of any material however simple from first principles must come from solving the Schrödinger Equation for a quantum many-body interacting system. As such, exact numerical solutions for such systems are empirical as per the size of the system. It therefore warrants that solutions to such systems be determined by approximations from time to time.

On the other hand, to determine the electronic properties of any given system in solid state physics, the Kohn-Sham equation within the Density Functional Theory using either Local spin density approximation or the generalized gradient approximation, which generally solves the many-body problem by considering a non-interacting systems with a one electron exchange correlation potential.

1.3 Problem statement.

Stannic rutile tetragonal SnO_2 is the largest ore of tin oxides and it is estimated to be about 99% abundant in the earth's crust. Furthermore SnO_2 is a transparent conducting metal oxide with numerous optoelectronic applications ranging from small scale to massive industrial usability. In this applications there is need to understand the theoretical predictions to open up the insight of the characteristics and properties of SnO_2. This work therefore will focus on the properties which will make SnO_2 an important optoelectronic solution to the growing demand for this class of materials.

1.4 RESEARCH OBJECTIVES.

1.40 GENERAL OBJECTIVES.

This project is aimed at establishing the structural properties of rutile tetragonal tin oxide and its electronic properties as well as its optical properties using LSDA calculations and y*ambo* coding computational methods.

1.41 SPECIFIC OBJECTIVES.

a) To determine the structural properties of rutile tetragonal SnO_2 using LSDA method.
b) To determine the electronic properties of rutile tetragonal SnO_2 using LSDA method.
c) To determine the optical properties of the body centered rutile tetragonal SnO_2 using GW and BSE methods.

1.5 JUSTIFICATION OF THE STUDY.

Of the oxides of tin, rutile stannous tin oxide is the most useful with stable structural, electrical and optical properties. It attracts dynamic applications owing to its conductivity and transparency in nature. Tin oxide is an attractive material due to its wide variety in its physical properties related to its electronic structure and optical nature. It is an n- type semiconductor with narrow band gap, making it to have a wide range of applications in solar energy, optics and electronics due to its absorbency, reflectivity and transmittance properties. Tin oxide has been under extensive theoretical and experimental research in the resent research world to date and there is

substantial information from these research findings describing the structure and electronic properties. Tin is one of the best transparent oxides, its optical properties have been studied extensively experimentally; in this studies however, this experimental results have not been tested theoretically. We seek to establish and proof the electronic, structural and optical properties of tin oxide using the theoretical techniques mainly by computational methods.

Treatment of correlations in metal oxides in the valence band has been a challenge and as such describing accurately the correlations in highly complex systems has proved to be a challenge. Hence it is still desirable to have more first – principles investigations of the electronic structure, optical properties and the mechanical structure of tin oxide using different approaches to enhance the understanding of tin oxide properties. LSDA is one such approach that works better for tin oxide and as a result, it gives better prediction of the electronic properties and mechanical structure. Tin oxide has many applications in solar energy, as such, studying it's optical properties using the GW and BSE methods of *yambo coding* becomes significant and crucial.

CHAPTER TWO.

2.0 LITERATURE REVIEW.

2.1 Introduction.

Tin oxide being a transparent metal oxide, it exhibits a wide range of physical properties related to its electronic structure. Its optical behavior forms the basis of a wide range of applications, as such, this material has been the subject of extensive experimental and theoretical investigations for the past years. In this chapter, we focus on the review of some of the essentials of tin oxide to set up the background in studying this material.

2.2 Experimental and Theoretical Structural and Electronic Studies.

Tin oxide occurs in two forms, stannous tin oxide (SnO) and Stannic tin oxide (SnO2). SnO does not have great electrical relevance and hence it has not spurred interest in the research world. Owing to its optoelectronic properties, SnO2 has been an extensive source of research. The figure below represents the structure of rutile tin oxide;

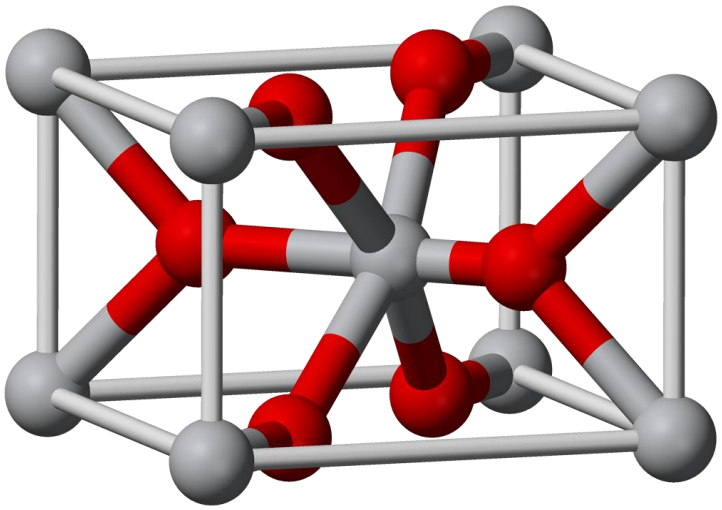

Fig. 1. Primitive unit cell of the bulk rutile structure, space group P4 2 mnm. white balls correspond to tin atoms, and red balls to the oxygen atoms. There are two units of SnO 2 in the unit cell.

The study of stannic tin oxide is motivated by its applications as a solid state gas sensor material[1], oxidation catalyst, and transparent conductor[3] due to its high photo stability and good carrier mobility [28,29]. The great diversity of oxide materials could not be better demonstrated than in the variety of self-assembled nanoscale materials that have been recently discovered. For tin oxide, for instance SnO nanodiskettes [5], SnO 2 nanobelts, and other nanoscopic materials [6] form. SnO 2 nanobelts have the bulk-like rutile structure . Their surfaces are low index bulk terminations and thus should exhibit similar properties to single crystal surfaces.

Many of these materials have gas sensing properties[5]. This and their large surface to volume ratio make them promising materials for well defined, highly sensitive gas sensors. The key for understanding many aspects of SnO 2 surface properties is the dual valency of Sn. The dual valency facilitates a reversible transformation of the surface composition from stoichiometric surfaces with Sn 4+ surface cations into a reduced surface with Sn 2+ surface cations depending on the oxygen chemical potential of the system[13]. Reduction of the surface modifies the surface electronic structure by formation of Sn 5s derived surface states that lie deep within the band gap and also cause a lowering of the work function[5]. In most applications tin oxide is modified by additives to either increase the charge carrier concentration by donor atoms, or to increase the gas sensitivity or the catalytic activity by metal additives. Some of the basic concepts by which additives modify the electronic structure of SnO2. The band gap of SnO2 has been determined to be 3.6eV[1,3,6].

2.3 Experimental and Theoretical Optical Studies.

The optical properties of rutile tetragonal stannic tin oxide have not been studied to a large extend [12]. The *Ab initio* calculations in the framework of density functional theory (DFT) [1] have yielded high-quality results for a large variety of systems, ranging from periodic solids to molecules and nanostructures [1]. These results are however mostly limited to quantities related to the ground state properties (structural and electronic), whereas additional phenomena that occur in the excited state are not correctly described [2].

Quantum-ESPRESSO is therefore not suitable for studying and describing the optical

properties of SnO2. *Yambo coding* has been extensively used to study the optical properties of SnO2. *Yambo coding* includes explicitly the electronic occupations, therefore *yambo* can be best applied to analyzing semiconductors, insulators and metals.

CHAPTER THREE.

3.0 THEORATICAL BACKGROUND.

3.1 STRUCTRURE OF MATERIALS

The structure of materials can be classified by the general magnitude of various features being considered. The three most common major classification of structural, listed generally in increasing size, are: Atomic structure, which includes features that cannot be seen, such as the types of bonding between the atoms, and the way the atoms are arranged [26]. Micro structure, which includes features that can be seen using a microscope, but seldom with the naked eye. Macro structure, which includes features that can be seen with the naked eye.

The atomic structure ideally affects the chemical, physical, thermal, electrical, magnetic, and optical properties of a material. The micro structure and macro structure can also affect these properties but they generally have a larger effect on mechanical properties and on the rate of chemical reaction of the material in question. The properties of a material open up the structure of the material [27]. This may be in line with the strength of metals, which in an engineering world may suggests that these atoms are held together by strong bonds and hence strong hints on the applicability of the material in the real world. To understand the structure of a material, the type of atoms present, and how the atoms are arranged and bonded must be known. For tin oxide for example, owing to its lucrative optoelectronic properties, a probe on its structure is important.

3.2 BAND STRUCTURE

The band structure of a solid describes the ranges of energy that an electron within the solid may have i.e the energy bands, allowed bands, or simply bands and ranges of energy that it may not have called band gaps or forbidden bands [18]. Band theory derives these bands and band gaps by examining the allowed quantum mechanical wave functions for an electron in a large, periodic lattice of atoms or molecules. Band theory has been successfully used to explain many physical properties of solids, such as electrical resistivity and optical absorption, and forms the foundation of the understanding of all solid state devices including; transistors, solar cells,

diodes and many others.

The existence of continuous bands of allowed energies can be understood starting with the atomic scale. The electrons of a single isolated atom occupy atomic orbitals, which form a discrete set of energy levels. If multiple atoms are brought together into a molecule, their atomic orbitals will combine to form molecular orbitals each with a different energy. In other words, n atomic orbitals will combine to form n molecular orbitals. As more and more atoms are brought together, the molecular orbitals extend larger and larger, and the energy levels of the molecule will become

increasingly dense. Eventually, the collection of atoms form a giant molecule, or otherwise commonly a solid. For this giant molecule, the energy levels are so close that they can be considered to form a continuum of states. {The fineness of spacing required to be considered an effective "continuum" depends on the situation.}

Band gaps are essentially leftover ranges of energy not covered by any band, a result of the finite widths of the energy bands. The bands have different widths, with the widths depending on the degree of overlap in the atomic orbitals from which they arise. Two adjacent bands may simply not be wide enough to fully cover the range of energy. For example, the bands associated with core orbitals such as 1s electrons are extremely narrow due to the small overlap between adjacent atoms. As a result, there tend to be large band gaps between the core bands. Higher bands involve larger and larger orbitals with more overlap, becoming progressively wider and wider at high energy so that there are no band gaps at high energy.

Band structure calculations take advantage of the periodic nature of a crystal lattice, exploiting its symmetry[9]. The single electron Schrödinger equation is solved for an electron in a lattice periodic potential, giving Bloch waves as solutions:

$$\psi_{nk}(r) = e^{ik\cdot r} U_{nk}(r) \qquad 1$$

where k is called the wave vector. For each value of k, there are multiple solutions to the Schrödinger equation labeled by n, the band index, which simply numbers the energy bands. Each of these energy levels evolves smoothly with changes in k, forming a smooth band of states. For each band we can define a function *E n (k)*, which is the dispersion relation for electrons in that band. The band gap of a semiconductor is always one of two types, a direct band

gap or an indirect band gap. The minimal energy state in the conduction band and the maximal energy state in the valence band are each characterized by a certain crystal momentum (k-vector) in the Brillion zone. If the k-vectors are the same, it is called a "direct gap". If they are different, it is called an "indirect gap". The band gap is called "direct" if the momentum of electrons and holes is the same in both the conduction band and the valence band; an electron can directly emit a photon. In an "indirect" gap, a photon cannot be emitted because the electron must pass through an intermediate state and transfer momentum to the crystal lattice [21].

Figure

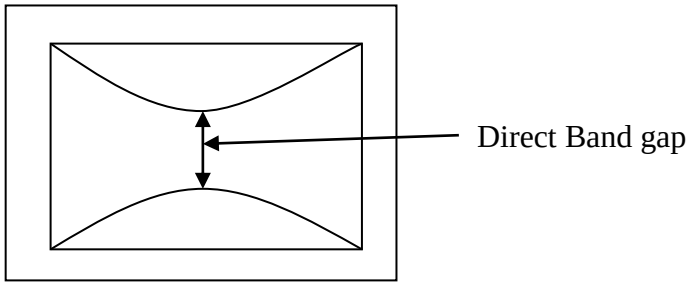

Figure

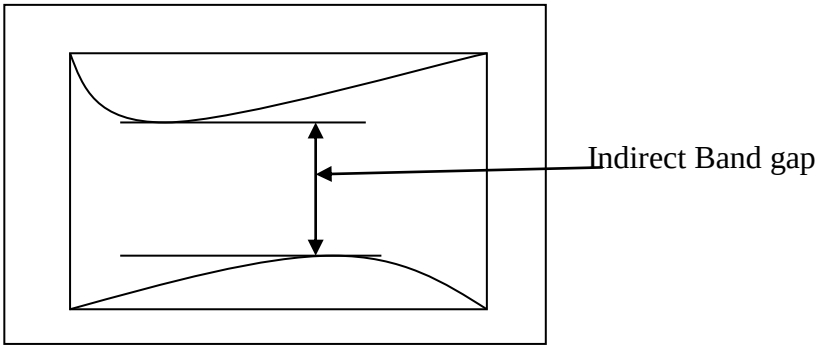

3.3 DENSITY OF STATES

Density of states (DOS) of a system describes the number of states per interval of energy at each energy level that are available to be occupied by electrons. Unlike isolated systems, like atoms or molecules in gas phase, the density distributions are not discrete like a spectral density but continuous. A high density of states at a specific energy level means that there are many states available for occupation. A density of states of zero means that no states can be occupied at that energy level. Generally a density of states is an average over the space

and time domains occupied by the system. Local variations, most often due to distortions of the original system, are often called local density of states (LDOS). If the density of states of an undisturbed system is zero, the local density of states can locally be non-zero due to the presence of a local potential [17].

The density of states in a semiconductor equals the density per unit volume and energy of the number of solutions to Schrödinger's equation. We will assume that the semiconductor can be mode led as an infinite quantum well in which electrons with effective mass, m * , are free to move. The energy in the well is set to zero. The semiconductor is assumed a cube with side L. This assumption does not affect the result since the density of states per unit volume should not depend on the actual size or shape of the semiconductor [18].

The solutions to the wave equation where *V(x)* = 0 are sine and cosine functions:

$$\psi = A \sin k_x \; x + B \cos k_x \; x \dots\dots\dots\dots\dots\dots\dots\dots\dots\dots\dots\dots\dots\dots\dots\dots\dots\dots\dots\dots\dots 2$$

Where A and B are to be determined. The wave function must be zero at the infinite barriers of the well. At x = 0 the wave function must be zero so that only sine functions can be valid solutions or B must equal zero. At x = L, the wave function must also be zero yielding the following possible value for the wave number, *k x* .

$$k_x = \frac{n\pi}{L}; \quad \{n = 1,2,3, \dots\dots\} \dots\dots\dots\dots\dots\dots\dots\dots\dots\dots\dots\dots\dots\dots\dots..3$$

This analysis can now be repeated in the y and z direction. Each possible solution then corresponds to a cube in k-space with size *np/L*. The total number of solutions with a different value for *k x* , *k y* and *k z* and with a magnitude of the wave vector less than *k* is obtained by calculating the volume of one eighth of a sphere with radius 21 *k* and dividing it by the volume corresponding to a single solution,, yielding:

$$N = 2 \times \frac{1}{8} \times \left(\frac{L}{\pi}\right)^3 \times \frac{4}{3} \times \pi k^3 \dots\dots\dots\dots\dots\dots\dots\dots\dots\dots\dots\dots\dots\dots\dots\dots 4$$

A factor of two is added to account for the two possible spins of each solution. The density per unit energy is then obtained using the chain rule:

$$\frac{dN}{dE} = \frac{dN}{dk}\frac{dk}{dE} = \left(\frac{L}{\pi}\right)^3 \pi k^2 \frac{dk}{dE} \dots\dots\dots\dots\dots\dots\dots\dots\dots\dots\dots\dots\dots..5$$

The kinetic energy E of a particle with mass m * is related to the wave number, k, by:

$$E_{(k)} = \frac{\hbar^2 k^2}{2m^*} \quad ; providing\ that\ \frac{dk}{dE} = \frac{m^*}{\hbar^2 k}\ \ and\ k = \frac{\sqrt{2m^* E}}{\hbar} \ldots\ldots\ldots\ldots\ldots\ldots\ldots 6$$

And the density of states per unit volume and per unit energy, $g(E)$, becomes:

$$g_{(E)} = \frac{1}{L^3}\frac{dN}{dE} = \frac{8\pi\sqrt{2}}{h^3} m^{*\frac{3}{2}}\sqrt{E}, \quad for\ E \gg 0 \ldots\ldots\ldots\ldots\ldots\ldots\ldots\ldots\ldots 7$$

The density of states is zero at the bottom of the well as well as for negative energies.

The same analysis also applies to electrons in a semiconductor. The effective mass takes into account the effect of the periodic potential on the electron. The minimum energy of the electron is the energy at the bottom of the conduction band, E c , so that the density of states for electrons in the conduction band is given by(33):

$$g_{c(E)} = \frac{8\pi\sqrt{2}}{h^3} m^{*3/2}\sqrt{E - E_c}, \quad for\ E \leq E_c \ldots\ldots\ldots\ldots\ldots\ldots\ldots\ldots\ldots\ldots\ldots\ldots\ldots\ldots\ldots\ldots\ldots 8$$

$$\boldsymbol{g_{c(E)} = 0, \qquad for\ E < E_c}$$

3.4 THEORY OF ELECTRONIC STRUCTURES

Electronic structure is the state of motion of electrons in an electrostatic field created by stationary nuclei.[19] The term encompass both the wave functions of the electrons and the energies associated with them. Electronic structure is obtained by solving quantum mechanical equations for the aforementioned clamped-nuclei problem. A number of methods to obtain electronic structures exist and their applicability varies from case to case[20]. The methods include:

- ✓ Born–Oppenheimer approximation
- ✓ Molecular Hamiltonian
- ✓ Schrödinger equation
- ✓ The Hartree Approximation
- ✓ Hartree-Fock Techniques

3.4.1 BORN–OPPENHEIMER APPROXIMATION

The computation of the energy and the wave function of an average size molecule is a formidable task that is alleviated by the Born–Oppenheimer (BO) approximation, named after Max Born and J. Robert Oppenheimer [21]. For instance the benzene molecule consists of 12 nuclei and 42 electrons. The time independent Schrödinger equation, which must be solved to obtain the energy and wave function of this molecule, is a partial differential eigenvalue equation in 162 variables the spatial coordinates of the electrons and the nuclei. The BO approximation makes it possible to compute the wave function in two less complicated consecutive steps

This approximation was proposed in 1927,[28] in the early period of quantum mechanics, by Born and Oppenheimer and is still indispensable in quantum chemistry. It allows the wave function of a molecule to be broken into its electronic and nuclear both vibrational and rotational components. In the first step of the BO approximation the electronic Schrödinger equation is solved, yielding

the wave function depending on electrons only. For benzene this wave function depends on 126 electronic coordinates[30]. During this solution the nuclei are fixed in a certain configuration, very often the equilibrium configuration. If the effects of the quantum mechanical nuclear motion are to be studied, for instance because a vibrational spectrum is required, this electronic computation must be in nuclear coordinates. In the second step of the BO approximation this function serves as a potential in a Schrödinger equation containing only the nuclei—for benzene an equation in 36 variables.

The success of the BO approximation is due to the high ratio between nuclear and electronic masses. The approximation is an important tool of quantum chemistry; without it only the lightest molecule, H 2 , could be handled, and all computations of molecular wave functions for larger molecules make use of it. Even in the cases where the BO approximation breaks down, it is used as a point of departure for the computations [28]

3.4.2 MOLECULAR HAMILTONIAN

In atomic, molecular, and optical physics and quantum chemistry, the molecular

Hamiltonian is the Hamiltonian operator representing the energy of the electrons and nuclei in a molecule. This operator and the associated Schrödinger equation play a central role in computational chemistry and physics for computing properties of molecules and aggregates of molecules, such as thermal conductivity, specific heat, electrical conductivity, optical, and magnetic properties, and reactivity [29].

The elementary parts of a molecule are the nuclei, characterized by their atomic numbers, Z, and the electrons, which have negative elementary charge, $-e$. Their interaction gives a nuclear charge of $Z + q$, where $q = -eN$, with N equal to the number of electrons. Electrons and nuclei are, to a very good approximation, point charges and point masses [15]. The molecular Hamiltonian is a sum of several terms: its major terms are the kinetic energies of the electrons and the Coulomb (electrostatic) interactions between the two kinds of charged particles. The Hamiltonian that contains only the kinetic energies of electrons and nuclei, and the Coulomb interactions between them, is known as the Coulomb Hamiltonian. From it is missing a number of small terms, most of which are due to electronic and nuclear spin.

Although it is generally assumed that the solution of the time independent Schrödinger equation associated with the Coulomb Hamiltonian will predict most properties of the molecule, including its shape (3D structure), calculations based on the full Coulomb Hamiltonian are very rare. The main reason is that its Schrödinger equation is very difficult to solve. Applications are restricted to small systems like the hydrogen molecule. Almost all calculations of molecular wave functions are based on the separation of the Coulomb Hamiltonian first devised by Born and Oppenheimer. The nuclear kinetic energy terms are omitted from the Coulomb Hamiltonian and one considers the remaining Hamiltonian as a Hamiltonian of electrons only. The stationary nuclei enter the problem only as generators of an electric potential in which the electrons move in a quantum mechanical way. Within this framework the molecular Hamiltonian has been simplified to the clamped nucleus Hamiltonian, also called electronic Hamiltonian that acts only on functions of the electronic coordinates.

Once the Schrödinger equation of the clamped nucleus Hamiltonian has been solved for a sufficient number of constellations of the nuclei, an appropriate eigenvalue preferably the lowest can be seen as a function of the nuclear coordinates, which leads to a potential energy surface. In practical calculations, the surface is usually fitted in terms of some analytic functions. In the second steps of the Born–Oppenheimer approximation the part of the full Coulomb Hamiltonian

that depends on the electrons is replaced by the potential energy surface. This converts the total molecular Hamiltonian into another Hamiltonian that acts only on the nuclear coordinates. In the case of a breakdown of the Born–Oppenheimer approximation—which occurs when energies of different electronic states are close—the neighboring potential energy surfaces are needed, see this article for more details on this.

The nuclear motion Schrödinger equation can be solved in a space-fixed (laboratory) frame, but then the translational and rotational (external) energies are not accounted for. Only the (internal) atomic vibrations enter the problem. Further, for molecules larger than triatomic ones, it is quite common to introduce the harmonic approximation, which approximates the potential energy surface as a quadratic function of the atomic displacements. This gives the harmonic nuclear motion Hamiltonian. Making the harmonic approximation, we can convert the Hamiltonian into a sum of uncoupled one-dimensional harmonic oscillator Hamiltonians. The one-dimensional harmonic oscillator is one of the few systems that allows an exact solution of the Schrödinger equation.

Alternatively, the nuclear motion (vibrational) Schrödinger equation can be solved in a special frame (an Eckart frame) that rotates and translates with the molecule. Formulated with respect to this body-fixed frame the Hamiltonian accounts for rotation, translation and vibration of the nuclei. Since Watson introduced in 1968 an important simplification to this Hamiltonian, it is often referred to as Watson's nuclear motion Hamiltonian, but it is also known as the Eckart Hamiltonian.

3.4.3 HARTREE FOCK THEORY

Hartree Fock theory is one of the simplest approximate theories for solving the many-body Hamiltonian [12]. It is based on a simple approximation to the true many-body wave function; that the wave function is given by a single Slater determinant of

spin-orbitals

$$\Psi_{Total} = \psi_{electronic} \times \psi_{nuclear} \dots\dots\dots\dots\dots\dots\dots\dots\dots\dots\dots\dots\dots\dots\dots\dots\dots\dots\dots\dots\dots\dots\dots\dots\dots\dots\dots 9$$

where the variables include the coordinates of space and spin. This simple ansatz for the wave function captures much of the physics required for accurate solutions of the Hamiltonian. Most

importantly, the wave function is ant symmetric with respect to an interchange of any two electron positions. This property is required by the Pauli Exclusion Principle, i.e.

$$\Psi = \begin{bmatrix} \psi_{1(x_1)} & \psi_{1(x_2)} & \cdots & \psi_{1(x_N)} \\ \psi_{2(x_1)} & \psi_{2(x_2)} & & \psi_{2(x_N)} \\ \vdots & & \ddots & \vdots \\ \psi_{N(x_1)} & \psi_{N(x_2)} & \cdots & \psi_{N(x_N)} \end{bmatrix} \ldots\ldots\ldots\ldots\ldots\ldots\ldots\ldots\ldots\ldots\ldots\ldots\ldots\ldots\ldots\ldots\ldots\ldots\ldots\ldots.10$$

This wave function may be inserted into the Hamiltonian, equation 10 and an expression for the total energy derived. [2,3,4] Applying the theorem that the value of a determinant is unchanged by any non-singular linear transformation, we may choose the ψ to be an orthonormal set. We now introduce a Lagrange multiplier to impose the condition that the ϵ are normalized, and minimize with respect to the $\boldsymbol{\psi}$

$$\psi_{(x_1, x_2, \ldots\ldots\ldots x_i \ldots\ldots, x_j \ldots\ldots\ldots\ldots, x_N)} = -\psi_{(x_1, x_2, \ldots\ldots x_j \ldots\ldots x_i \ldots\ldots x_N)} \ldots\ldots\ldots\ldots\ldots\ldots\ldots\ldots\ldots\ldots\ldots..11$$

An enormous simplification of the expressions for the orbitals results. They reduce to a set of one-electron equations of the form

$$\delta/_{\delta\psi}\left[< \hat{H} > - \sum_j \epsilon_j \int \left|\psi_j\right|^2 dr\right] = 0 \ \ldots\ldots\ldots\ldots\ldots\ldots\ldots\ldots\ldots\ldots\ldots\ldots\ldots\ldots.12$$

where ϵ is a non-local potential and the local ionic potential is denoted by V_{ions}. The one-electron equations resemble single-particle Schrödinger equations.

The full Hartree Fock equations are given by

$$\begin{aligned} \epsilon_i \psi_{i(r)} &= \left(-\frac{1}{2}\nabla^2 + V_{ions(r)}\right)\psi_{i(r)} \\ &\quad + \sum_j \int d\,r' \frac{\left|\psi_{j(r')}\right|^2}{|r - r'|}\psi_{i(r)} \\ &\quad - \sum_j \delta_{\sigma_i \sigma_j} \int dr' \frac{\psi^*_{j(r')}\psi_{i(r')}}{|r - r'|}\psi_{j(r)} \ldots\ldots\ldots\ldots\ldots\ldots\ldots.13 \end{aligned}$$

The right hand side of the equations consists of four terms. The first and second give rise to the kinetic energy contribution and the electron-ion potential. The third term, or Hartree term, is the simply electrostatic potential arising from the charge distribution of term includes an unphysical

self-interaction of N electrons . As written, the term includes an unphysical self-interaction of electrons when $j = i$.

This term is canceled in the fourth, or exchange term. The exchange term results from our inclusion of the Pauli principle and the assumed determinant form of the wave function [24]. The effect of exchange is for electrons of like-spin to avoid each other. Each electron of a given spin is consequently surrounded by an ``exchange hole", a small volume around the electron which like-spin electron avoid. The Hartree-Fock approximation corresponds to the conventional single-electron picture of electronic structure: the distribution of the electron distributions electrons is given simply by the sum of one .

This allows concepts such as labeling of electrons by angular momenta (`` a 3d electron in a transition metal"), but it must be remembered that this is an artifact
of the initial ansatz and that in some systems modifications are required to these ideas. Hartree-Fock theory, by assuming a single-determinant form for the wave function, neglects correlation between electrons. The electrons are subject to an average non-local potential arising from the other electrons, which can lead to a poor description of the electronic structure. Although qualitatively correct in many materials and compounds, Hartree-Fock theory is insufficiently accurate to make accurate quantitative predictions.

3.4.4 POST-HARTREE–FOCK

Post-Hartree–Fock [25,26] methods are the set of methods developed to improve on the Hartree– Fock (HF), or self-consistent field (SCF) method. They add electron correlation which is a more accurate way of including the repulsions between electrons than in the Hartree–Fock method where repulsions are only averaged.

Generally, the SCF procedure makes several assumptions about the nature of the multi-body Schrödinger equation and its set of solutions: -

- ✓ The Born–Oppenheimer approximation is inherently assumed. The true wave function should also be a function of the coordinates of each of the nuclei.
- ✓ Typically, relativistic effects are completely neglected. The momentum operator is assumed to be completely non relativistic.

- ✓ The basis set is composed of a finite number of orthogonal functions. The true wave function is a linear combination of functions from a complete (infinite) basis set.
- ✓ The energy eigenfunctions are assumed to be products of one-electron wave functions. The effects of electron correlation, beyond that of exchange energy resulting from the anti-symmetrization of the wave function, are completely neglected.

For the great majority of systems under study, in particular for excited states and processes such as molecular dissociation reactions, the fourth item is by far the most important. As a result, the term post-Hartree–Fock method is typically used for methods of approximating the electron correlation of a system. Usually, post-Hartree–Fock methods give more accurate results than Hartree–Fock calculations, although the added accuracy comes with the price of added computational cost.

3.5 DENSITY FUNCTIONAL THEORY

Density functional theory (DFT) is a powerful, formally exact theory and references within. It is distinct from quantum chemical methods in that it is a non-interacting theory and does not yield a correlated many-body wave function. In the Kohn-Sham DFT, the theory is a one-electron theory and shares many similarities with Hartree-Fock[27]. DFT has come to prominence over the last decade as a method potentially capable of very accurate results at low cost. In practice, approximations are required to implement the theory, and a significantly variable accuracy results. Calibration studies are therefore required to establish the likely accuracy in a given class of systems.

In recent physics literature, a large majority of the electronic structures and band plots are calculated using density functional theory (DFT), which is not a model but rather a theory, i.e., a microscopic first principles theory of condensed matter physics that tries to cope with the electron-electron many-body problem by the introduction of an exchange-correlation term in the functional of the electronic density. Density functional theory calculated bands are in many cases found to be in agreement with experimentally measured bands, for example by angle resolved

photo emission spectroscopy (ARPES). In particular, the band shape is typically well reproduced by DFT. But there are also systematic errors in DFT bands when compared to experiment results. In particular, DFT seems to systematically underestimate by about 30-40% the band gap in insulators and semiconductors [28].

It is commonly believed that DFT is a theory to predict ground state properties of a system only (e.g. the total energy, the atomic structure, etc.), and that excited state properties cannot be determined by DFT. This is a misconception. In principle, DFT can determine any property (ground state or excited state) of a system given a functional that maps the ground state density to that property. This is the essence of the Hohenburg–Kohn theorem. In practice, however, no known functional exists that maps the ground state density to excitation energies of electrons within a material [18]. Thus, what in the literature is quoted as a DFT band plot is a representation of the DFT Kohn–Sham energies, i.e., the energies of a fictive non-interacting system, the Kohn– Sham system, which has no physical interpretation at all.

The Kohn–Sham electronic structure must not be confused with the real, quasi particle electronic structure of a system, and there is no Koopmans's theorem holding for Kohn–Sham energies, as there is for Hartree–Fock energies, which can be truly considered as an approximation for quasi particle energies. Hence, in principle,

Kohn–Sham based DFT is not a band theory, i.e., not a theory suitable for calculating bands and plotting band. In principle time dependent DFT can be used to calculate the true band structure although in practice this is often difficult. A popular approach is the use of hybrid functional, which incorporate a portion of Hartree–Fock exact exchange; this produces a substantial improvement in predicted band gaps of semiconductors, but is less reliable for metals and wide-band gap materials.

3.6 BETHE SALPETER EQUATION {BSE}

The BSE is used to treat the excitation effects introduced by the electron-hole Green's function L.it can be obtained from Hedin's Equations and this can be written as follows;

$$L = L_0 + L_0\left(v + i\frac{\delta\Sigma}{\delta G}\right)L \ldots\ldots\ldots\ldots\ldots\ldots\ldots\ldots\ldots\ldots\ldots\ldots\ldots\ldots\ldots\ldots\ldots\ldots\ldots\ldots\ldots\ldots 14$$

making substitutians and rearranging the above equation, the self energy in equation 14 can be written as follows;

$$L = L_0 + L_0\left(v - \frac{\delta GW}{\delta G}\right)L = L_0 + L_0\left[v - \left(W - \frac{\delta W}{\delta G}\right)\right]L \ldots\ldots\ldots\ldots\ldots\ldots\ldots\ldots\ldots\ldots\ldots\ldots 15$$

The variation of the screened Coulomb interaction (W) with respect to the Dyson equation *(G)* tends to zero and hence 15 can be written as follows;

$$L = L_0 + L_0(v - W)L \ldots\ldots\ldots\ldots\ldots\ldots\ldots\ldots\ldots\ldots\ldots\ldots\ldots\ldots\ldots\ldots\ldots\ldots\ldots\ldots\ldots\ldots 16$$

the above equation 16 is commonly known as the BSE and it describes the coupled propagation of two particles including the electron and the hole.

CHAPTER FOUR.

4.0 METHODOLOGY

4.1 Introduction

In this study, the calculations on the ground state properties for SnO2 were done using Quantum-ESPRESSO coding [30]. This is an integrated suit of computation code for electronic structure calculations and material modeling which is based on density functional theory (DFT), plane waves and pseudo potentials (ultra soft, norm-conserving, projector-augmented wave). The optical properties were studied using *yambo code* [32]. This is an *ab initio* code for calculating quasi particle energies and optical properties of electronic systems within the framework of many-body perturbation theory and the time-dependent density functional theory.

4.2 QUANTUM ESPRESSO

Quantum-ESPRESSO is a software suite for *ab initio* quantum chemistry methods of electronic structure calculation and materials modeling, distributed for free under the GNU General Public License which works well in Linux, Ubuntu and Kubuntu. It is based on density functional theory (DFT), plane wave basis sets and pseudo potentials (ultra soft, norm-conserving, projector-augmented wave) . ***ESPRESSO*** is an acronym for op***E***n-***S***ource ***P***ackage for ***R***esearch in ***E***lectronic ***S***tructure, ***S***imulation, and ***O***ptimization [30]. The structural properties and electronic properties of SnO2 where done using this coding software. Quantum-ESPRESSO can be used in performing the following:

- ✓ Self-consistent, plane wave, pseudo potential total energy calculation
- ✓ Pseudo potential generation code and pseudo potential library
- ❖ Norm-conserving, ultra soft and projector-augmented wave.
- ❖ Scalar relativistic, fully relativistic
  - ➢ Geometric optimization also with variable cells .
- ✓ Inclusion of electric field, macroscopic polarizability
- ✓ Non collinear magnetism
- ✓ Infrared and Raman cross sections

- ✓ Dielectric tensors
- ✓ Meta dynamics
- ✓ Ballistic conductance
- ✓ Maximally localized Wannier functions
- ✓ Nudged Elastic Bands

In this study Quantum-ESPRESSO was able to do structural optimization, Self consistent and non self consistent total energy calculations, density of states (DOS) and projected density of states (PDOS).

4.3 DENSITY FUNCTIONAL THEORY (DFT) FORMALISM.

For purpose of studying the ground state properties of electronic systems for the quantum many-body problems, we engage in describing the Hamiltonian for the interaction between the electrons which are identical Fermionic particles. This complex many-body problem is reduced to solving the simpler problems of a single non-interacting electron moving in an effective field. In Density Functional Theory [30], the ground state energy of a system is obtained from the ground state electron density. Extensive approximations including the LDA, GGA, LSDA and LSDA+U, have allowed practical and quantitatively accurate calculations for ground-state properties to be made using DFT.

4.4 PSEUDO-POTENTIALS

The pseudo potentials used in this study were Norm-conserving pseudo potentials for both Sn and O. The pseudo potentials used were as follows:-

Sn Sn.pbe-hgh.UPF

O O.pbe-hgh.UPF

The pseudo potentials used had the following specifications for the outer most electrons:-

4.5 STRUCTURE OPTIMIZATION.

In this study, DFT was used to do the following computations:

- ✓ Running the relaxation calculation.
- ✓ Self consistent plane wave function (scf) calculations mainly in k points, cut off energy optimization and cell dimensions.
- ✓ Non-consistent plane wave function(nscf) calculations for the band structure
- ✓ Running the bands calculations that were applied in plotting of band structure.
- ✓ Density of states calculations
- ✓ Projected density of states calculations.

Xcryden was used to study structural properties k-path selection.
Xmgrace and *gnuplot* were used in plotting the graphs for cell dimension optimization, band structure, density of states and projected density of states.

For the plane wave pseudo potential calculations done, attention was put on cutoff energy convergence;the cutoff for wave-function expansion and the number of k points which measures how well the discrete grid had approximated the continuous integral over Brillion Zones (BZ). The higher the cutoffs, the higher the accuracy, however, time should also be considered as stated earlier,since this high cutoff calculations will take longer to run.

4.5.0 K-POINTS OPTIMIZATION PROCEDURE

Being a tetragonal rutile structured material, Optimization of k-points was not very necessary but however the optimization considered variation of points from 2,3,4,5,6,7, 8 and 9 and then executed using the running command *pw.x <input-file.in> output-file.out* . A table of variation in energy and selected k-points using *grep* command and from this table, a graph of energy against k-points was generated using *xmgrace* and *gnuplot* command. From the graph, one of the k-points was selected a point where the graph was constant.

4.5.1 CUTOFF ENERGY OPTIMIZATION PROCEDURE

I considered the optimized value of k-points selected and varied cutoff energy from 20-120 and using the *pw.x* command and *grep*, the values found were put in a file from which a graph of *xmgrace* and *gnuplot* drawn. From the graph, the best cutoff energy was chosen mainly from where the graph was constant accuracy and time considered.

4.5.2 CELL DIMENSIONS OPTIMIZATION PROCEDURE

With the optimized values of k-points and ecut I varied cell dimension against total energy by running the input file by *scf* calculations. Being a tetragonal structure, a=b=c, it has cell dimensions 1 and 3. For all the dimensions a table of energy variation with cell dimension was created using *grep* command. Graphs of total energy verses cell dimensions plotted using *xmgrace* and *gnuplot* for the two phases. The point with minimum total energy was chosen since this is the point where the system is stable.

4.6 ELECTRONIC PROPERTIES.

4.6.0 PROCEDURE FOR RUNNING SCF CALCULATIONS

After cell optimization for the two phases, i.e. k-points, cutoff energy, cell optimization, the chosen values were used to run *scf* calculations using *pw.x* command. The output file gave Fermi energies and total energies for the two phases.

4.6.1 PROCEDURE FOR RUNNING NSCF CALCULATIONS

The input files that were used in the above were copied to other files with *nscf. in* extension. In the input file with *nscf. in*, the following adjustments were done:

- ✓ calculation changed to '*nscf*'

- ✓ occupation changed to 'tetrahedra' from 'smearing'
- ✓ number of bands included in the systems block
- ✓ The number of k-points where increased by a factor of 3.

I ran the *nscf.in* file using the *pw.x* command.

4.6.2 PROCEDURE FOR BAND STRUCTURE COMPUTATIONS

The structure of the optimized cell was displayed by *Xcrysden* using suitable k-paths. The results were saved in a file with extension *pwscf*. The optimized input file was copied to another folder called bands and using cat *file.pwscf*>> optimized input file was used to replace the k-points initially optimized with new k-points from the *file.pwscf*. The new input file was edited to remove the initial k-points. The calculation part was changed to 'bands and the new file copied to *file-bands.in* keeping the prefixes for each *file. pw.x* command was used to run optimized *inputfile.in* followed by *band.x<bands.in>bands.out* to calculate the band structure. I used *plotband.x* and provided input file, output file,choose the range of energy and Fermi energy , plotting values from which a link to *xmgrace* was given and the band structure plotted with *xmgrace* and *gnuplot*.

4.6.3 COMPUTATION OF DENSITY OF STATES

Dos.in file was created that had the following content :

The files were ran using *dos.x <dos.in> dos.out* from which I got the *dos.dat* file that was used to plot the dos graph using *xmgrace* and *gnuplot.*

4.6.4 COMPUTATION OF PROJECTED DENSITY OF STATES

A file of *pdos.in* was created that had the following content:

The file was run using the *projwf.x* command as follows; *projwfc.x<pdos.in>pdos.out.* The results were wave functions for each state of Sn atoms and O atoms. I used *xmgrace* to plot the graphs for the states.

CHAPTER FIVE.
5.0 RESULTS AND DISCUSSIONS.

5.1 STRUCTURAL PROPERTIES OF SnO2.

Tin oxide (TO) is an attractive transparent conductor since it is less expensive and scarce compared to indium [3,5,12]. Rutile tin oxide crystallizes in a tetragonal structure with space group D4h P4 2 /mnm [3]. The unit cell is rutile tetragonal, with six atoms two stannous and four oxygen atoms [3]. Each tin atom is at the center of six oxygen atoms placed approximately at the corners of a regular slightly deformed octahedron, and three tin atoms approximately at the corners of an equilateral triangle surround every oxygen atom and is characterized by the lattice parameters a and c and intrinsic parameter u. The atoms of Sn are located in the bcc-positions (0, 0, 0) and (1/2, 1/2, 1/2) and are surrounded by oxygen atoms being in the positions ± (u, u, 0) and ± (1/2+u, 1/2–u, 1/2) [1,2,3] to form a distorted tetrahedron. The optimized cell parameters obtained in the calculation are a=b= 4.738Å, c= 3.188Å and u = 0.30756 [1,4]. In the bulk all Sn atoms are six fold coordinated to threefold coordinate oxygen atoms. . A unit cell with lattice constants a=b= 4.7374(1) Å and c = 3.1864(1) Å contains two tin and four oxygen atoms. The tin cations are located at the a sites, and the oxygen anions are found at the f sites, according to Wyckoff notation. From the oxygen perspective, the tin atoms are located at approximately the corners of an equilateral triangle.

The study of rutile tin oxide was done by examining its electronic properties using quantum espresso code and its optical properties are investigated using *yambo* code. Quantum ESPRESSO is a software suite for *ab initio* quantum chemistry methods of electronic structure calculation and materials modeling. It is based on density functional theory, plane wave basis sets, and uses pseudo potentials. Electronic structure of the rutile SnO2 was done by this powerful computation software. In this study, quantum ESPRESSO was able to do geometric optimization,Self-consistent (scf) and non self-consistent (nscf) total energy calculations, density of states and projected density of states.

5.2 ELECTRONIC PROPERTIES FOR SnO2.

The optimization of Sn2O was done using the following input file.

```
&control
    restart_mode='from_scratch',
    calculation='scf',
    outdir = './',
    pseudo_dir='/home/masika/Applications/espresso-5.0.2/pseudo',
    prefix = 'Sn2O',
/
&SYSTEM
    ibrav=6,
    celldm(1)= 9.3,
    celldm(3)= 0.684,
    nat=  6, ntyp= 2,
    ecutwfc =100 ,
    ecutrho = 400,
    occupations='smearing',
    smearing='marzari-vanderbilt',
    degauss=0.05
/
&ELECTRONS
     mixing_mode = 'plain',
     mixing_beta = 0.7,
     conv_thr = 1.0e-8,
/
ATOMIC_SPECIES
Sn 50.011 Sn.pbe-hgh.UPF
O  15.9994 O.pbe-hgh.UPF
ATOMIC_POSITIONS {crystal}
Sn      0.000000000   0.000000000   0.000000000
```

Sn 0.500000000 0.500000000 0.500000000

O 0.313000000 0.313000000 0.000000000

O 0.813000000 0.187000000 0.500000000

O -0.313000000 -0.313000000 0.000000000

O -0.813000000 -0.187000000 0.500000000

K_POINTS automatic

6 6 9 0 0 0

The pseudo potentials used in this study were NORM-OCONSERVING Sn.pbe-dn-kjpaw_psl.0.2.UPF and O.pbe-n-rrkjus_psl.0.1.UPF. The pseudo potential for Sn used has the following valence and occupation specifications:

Valence configuration:

nl	pn	l	occ	Rcut	Rcut US	E pseu
5S	1	0	2.00	2.000	2.200	-0.775326
5P	2	1	2.00	2.300	2.500	-0.271510
4D	3	2	10.00	1.700	2.400	-1.899141

Generation configuration:

5S	1	0	2.00	2.000	2.200	-0.775324
5S	1	0	0.00	2.000	2.200	3.100000
5P	2	1	2.00	2.300	2.500	-0.271509

5P 2 1 0.00 2.300 2.500 6.300000

4D 3 2 10.00 1.700 2.400 -1.899141

4D 3 2 0.00 1.700 2.400 4.300000

As compared to the electronic configuration of Sn the valence occupation of the pseudo potential used agrees with the electronic configuration of the element Sn

5.3 DFT CALCULATIONS FOR RUTILE TIN OXIDE (SnO2)

5.3.1 K-POINTS OPTIMIZATION

SnO2 is a rutile tetragonal structure whose k-points can be obtained most preferably by calculation but can also be obtained by optimization which I did by variation from 2,3,4,5,6,7,8 and 9. I then plotted the graph below which agrees with the theoretical calculations.
By calculation,

$$x = y = 1/a$$

$$= 1/4.737$$

$$= 0.21x10$$

$$= 2x3$$

$$x, y = 6,6$$

$$z = 1/c = 1/3.181$$

$$= 0.31x10$$

$$= 3x3$$

$$z = 9$$

$$(x, y, z) = (6, 6, 9)$$

therefore the values of k-points can be taken to be any multiple of this. For my calculations I took the value to be (6,6,9) which coincides with the optimized value as shown by the k-points graph below.

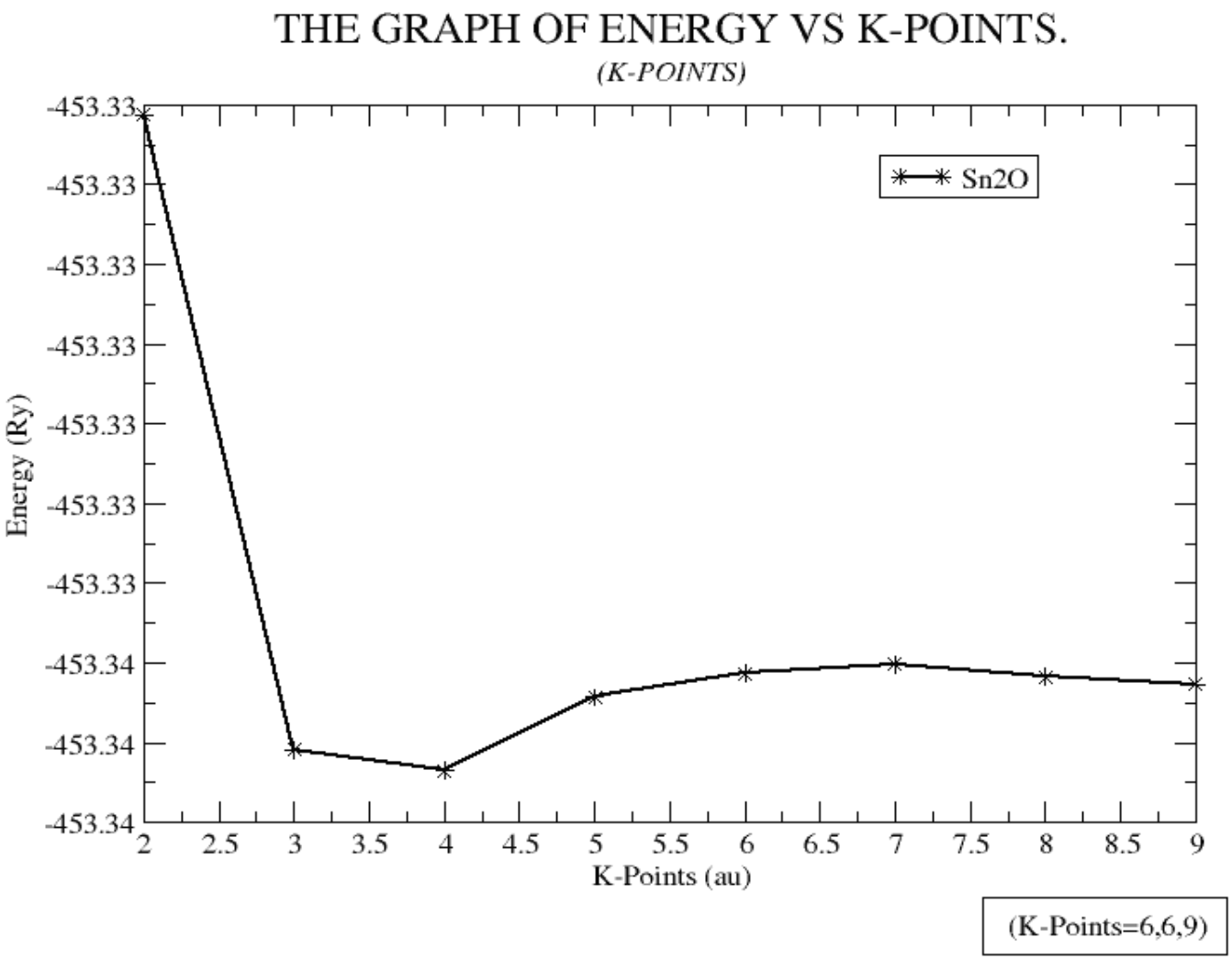

Fig.2: the graph of energy Vs k-points.

5.3.2 KINETIC ENERGYCUT OFF (ECUT) OPTIMIZATION

I considered the value of k-points as obtained from the optimization process of k-points above as (6,6,9) and I varied cutoff energy from 20 to 105Ry to get the optimized value of ecut as 75Ry as shown by the graph below.

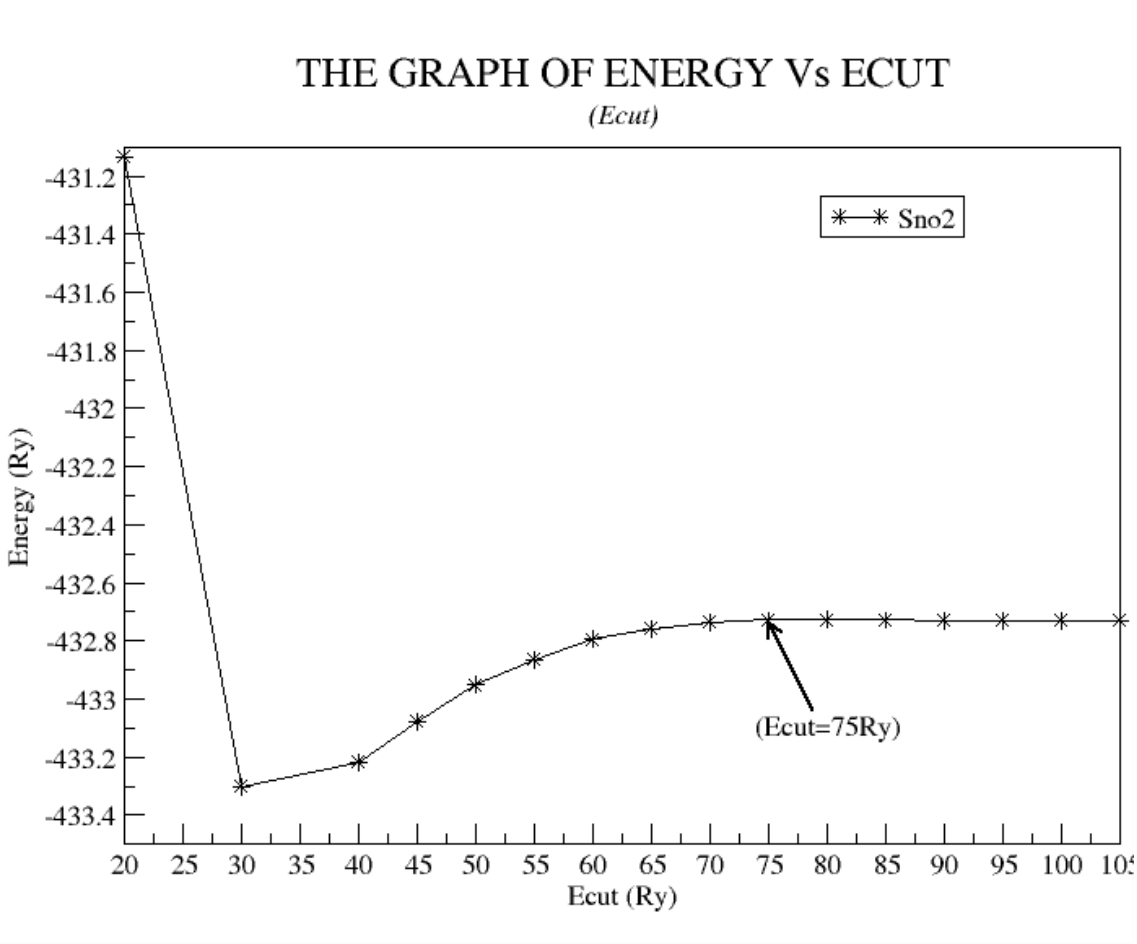

Fig.3 The graph energy against the kinetic energy cut off.

5.3.3 CELL DIMENSIONS (celldm1 & celldm3) OPTIMIZATION.

Being a tetragonal structure, $a = b \neq c$, the SnO2 rutile structure has two cell dimensions, celldm1 and celldm3. I retained the optimized value for k-points and the value obtained for the ecut. I first optimized for celldm1 by varying the value for celldm1 for values of celldm1 ranging from 8.6au to 11au and then plotted the value of the total energy against the celldm1. The experimental value of celldm1 is 8.9496au, however from the graph below; the optimized value of celldm1 was obtained as 9.2au which represents an error of 6.98%.

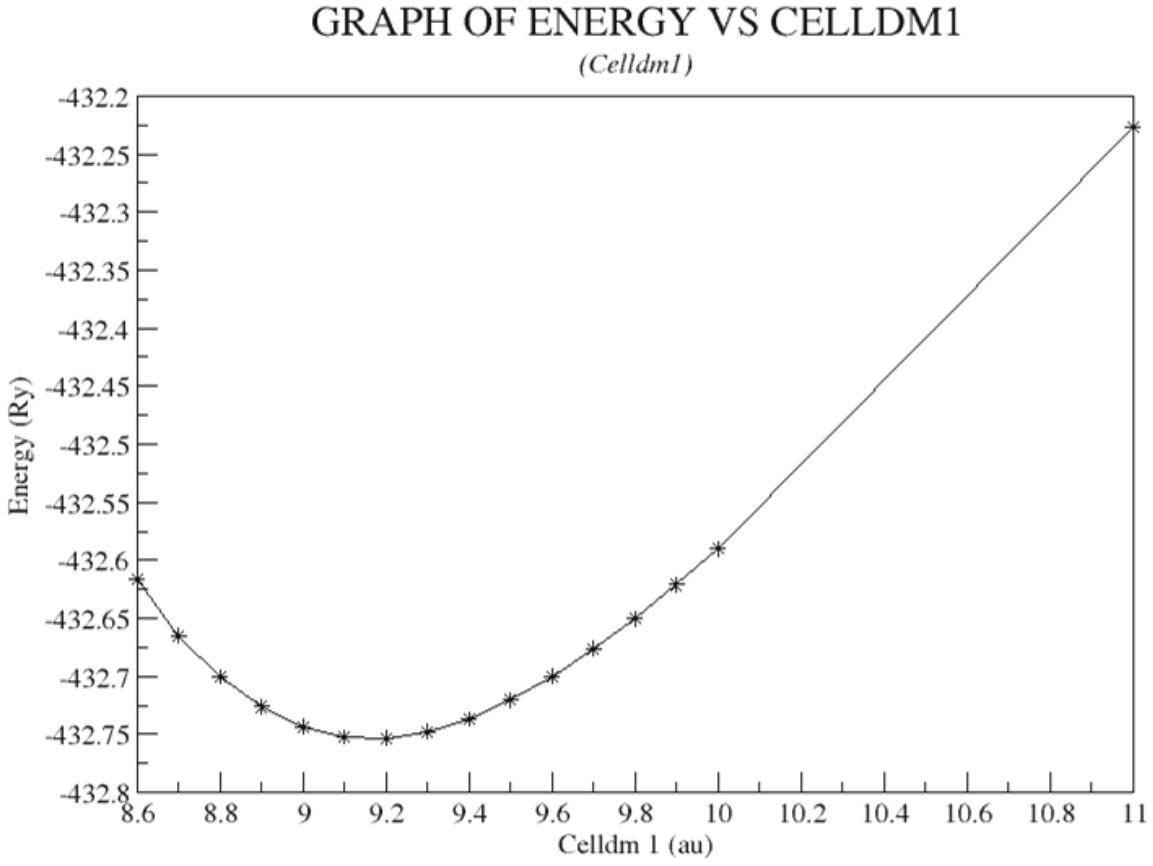

Fig.4: The graph of Energy against cell dimension one (celldm1).

Similarly I varied the values for celldm3 for values ranging from 0.64au to 0.75au and then plotted the value of the total energy against the celldm3. The experimental value of the celldm3 is given as 0.67au, however from the graph below, the optimized value of 0.70au was obtained which agrees with the experimental value giving an error of 4.48%.

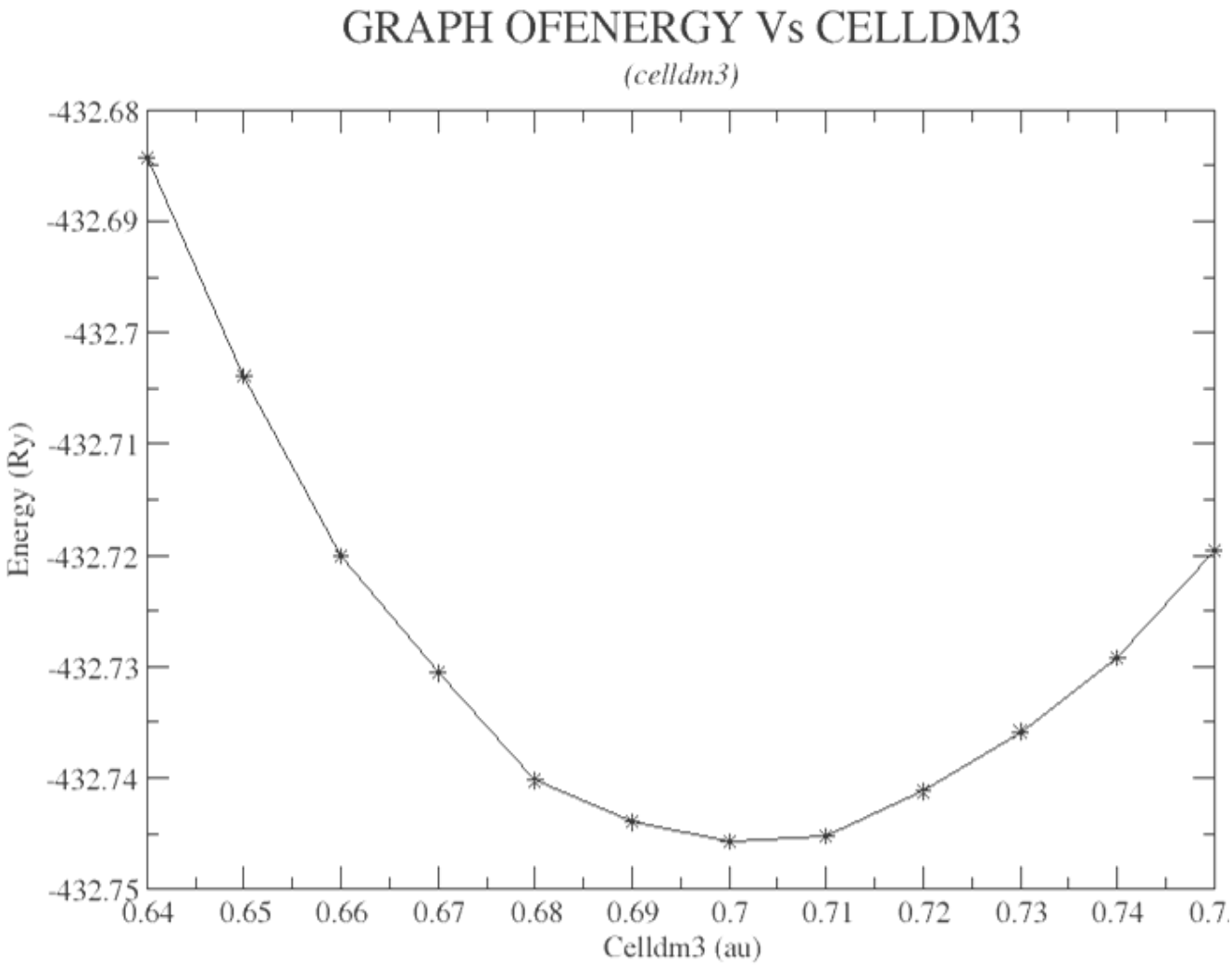

Fig.5: The graph of Energy against cell dimension three (celldm3).

5.3.4 RUNNING SCF CALCULATIONS

After cell optimization for the K-points, ecut, celldm1 and celldm3, our cell parameters have now been determined and therefore we can run the scf, nscf, bands calculations, dos and pdos. The output for the scf calculation gives the Fermi energy to be 4.6650 eV. When the bands where plotted, the evident band structure shows band gap of 3.52eV between the conduction and valence bands as shown the graph below. This shows a variation of 2.22% from the largely quoted theoretical value of 3.6eV.

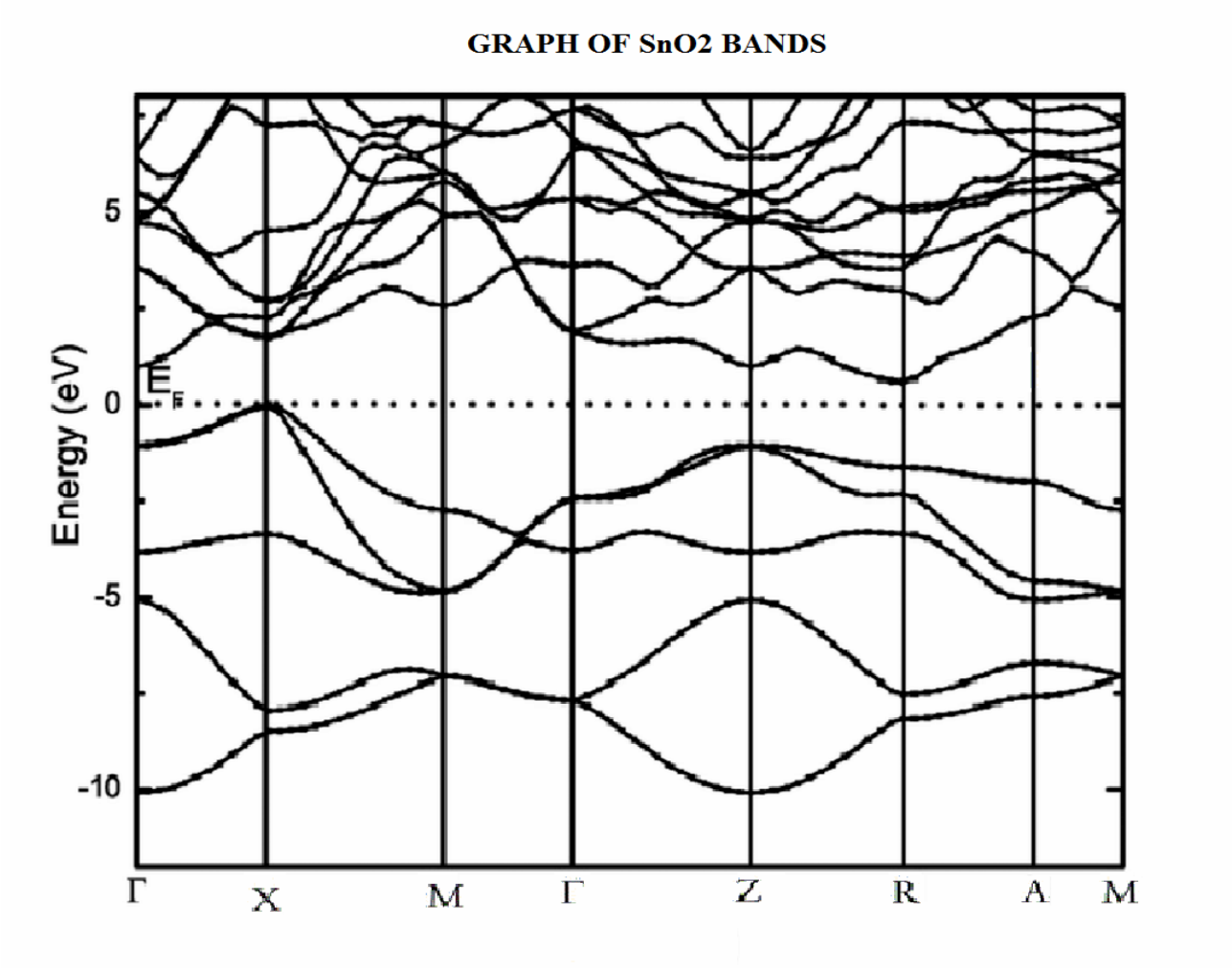

Fig.6: The figure shows the graph of Energy against the symmetric points for the k-points.

5.3.5 DENSITY OF STATES (dos) COMPUTATION

I created a Dos.in input file and I ran the file using the following command:

dos.x <dos.in> dos.out

This gave me the *dos.dat* file which I used to plot the dos graph using xmgrace. The dos graph obtained were as shown below.

From the graph the structure of SnO2 can be presumed to be having a very small band gap between the valence and conduction bands.

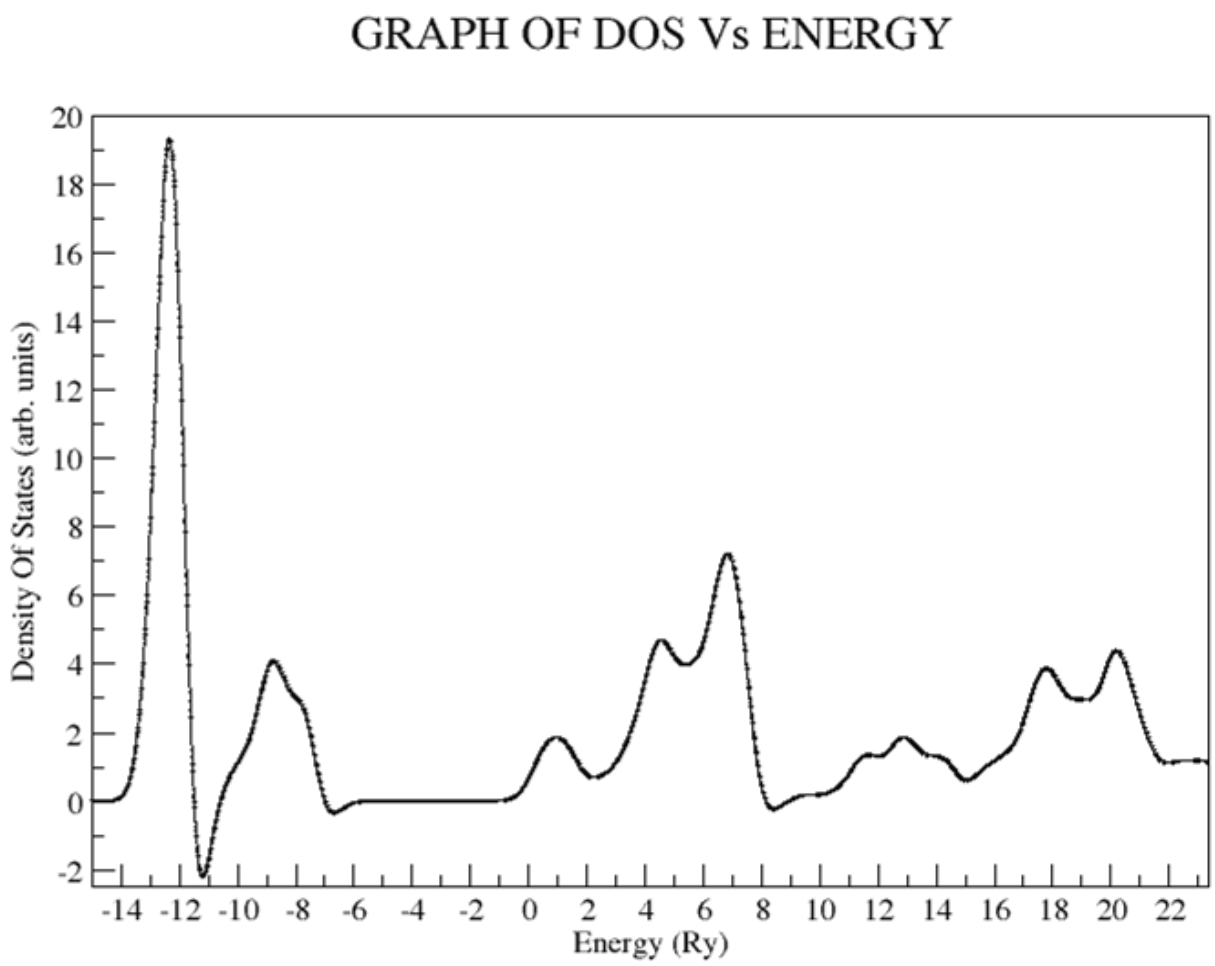

Fig. 7: The figure represents the graph the density of states plotted against the energy.

5.3.6 PROJECTED DENSITY OF STATES (pdos) COMPUTATION

The pdos.in file was created and run using the projwf.x command as follows;

projwfc.x<pdos.in>pdos.out.

The results obtained were wave functions for each state of tin atoms and Oxygen atoms. I used *xmgrace* to plot the graphs for the states the output graph was as shown below. The oxygen atoms are responsible for the reduced band gap since they are the most participating atoms around the Fermi level as seen from the graph of *pdos* below.

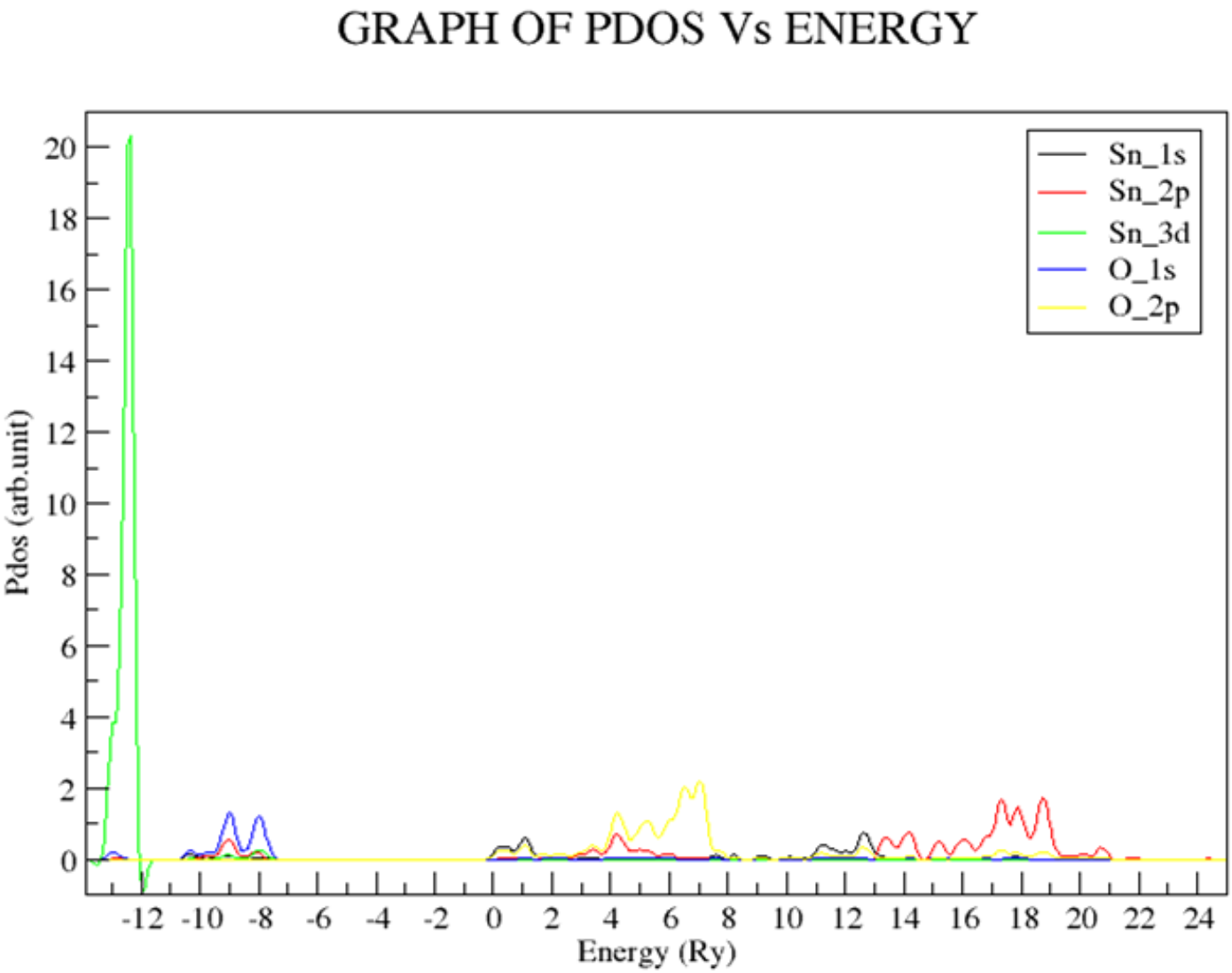

Fig.8: The graph of projected density of states plotted against the total Energy.

To visualize and understand the electronic properties for the rutile tetragonal SnO2 results as obtained from the DFT calculation I superimposed the graphs of dos and bands and then dos, pdos and bands as shown in the fig.9a and 9b below.

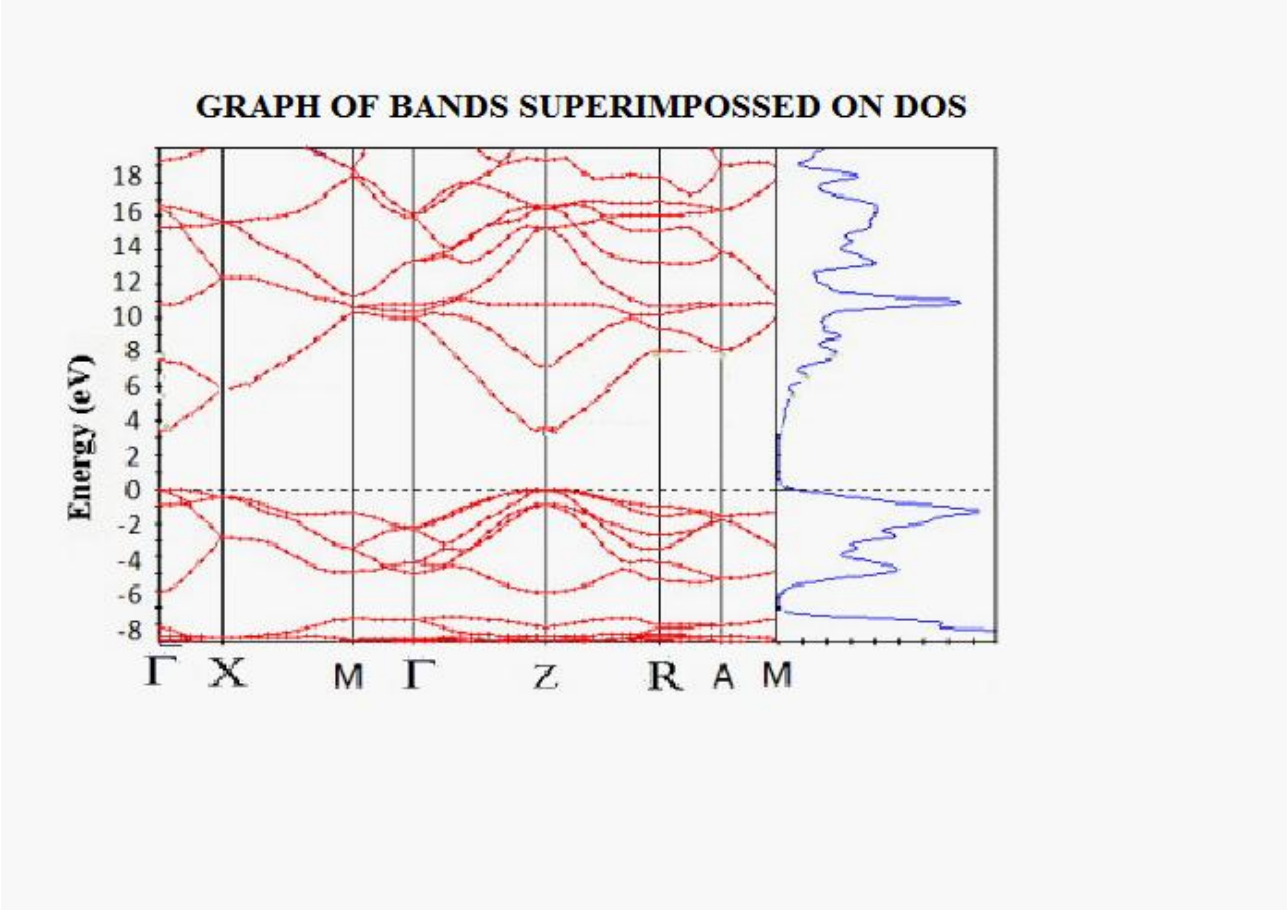

Fig.9a: Graph of dos superimposed on bands.

The above graph shows that at the Fermi level, SnO2 has a band gap as predicted by the theocratic and experimental studies. This is a very powerful characteristic for these conducting oxides. This implies that as per these results SnO2 is good conducting metal oxide.

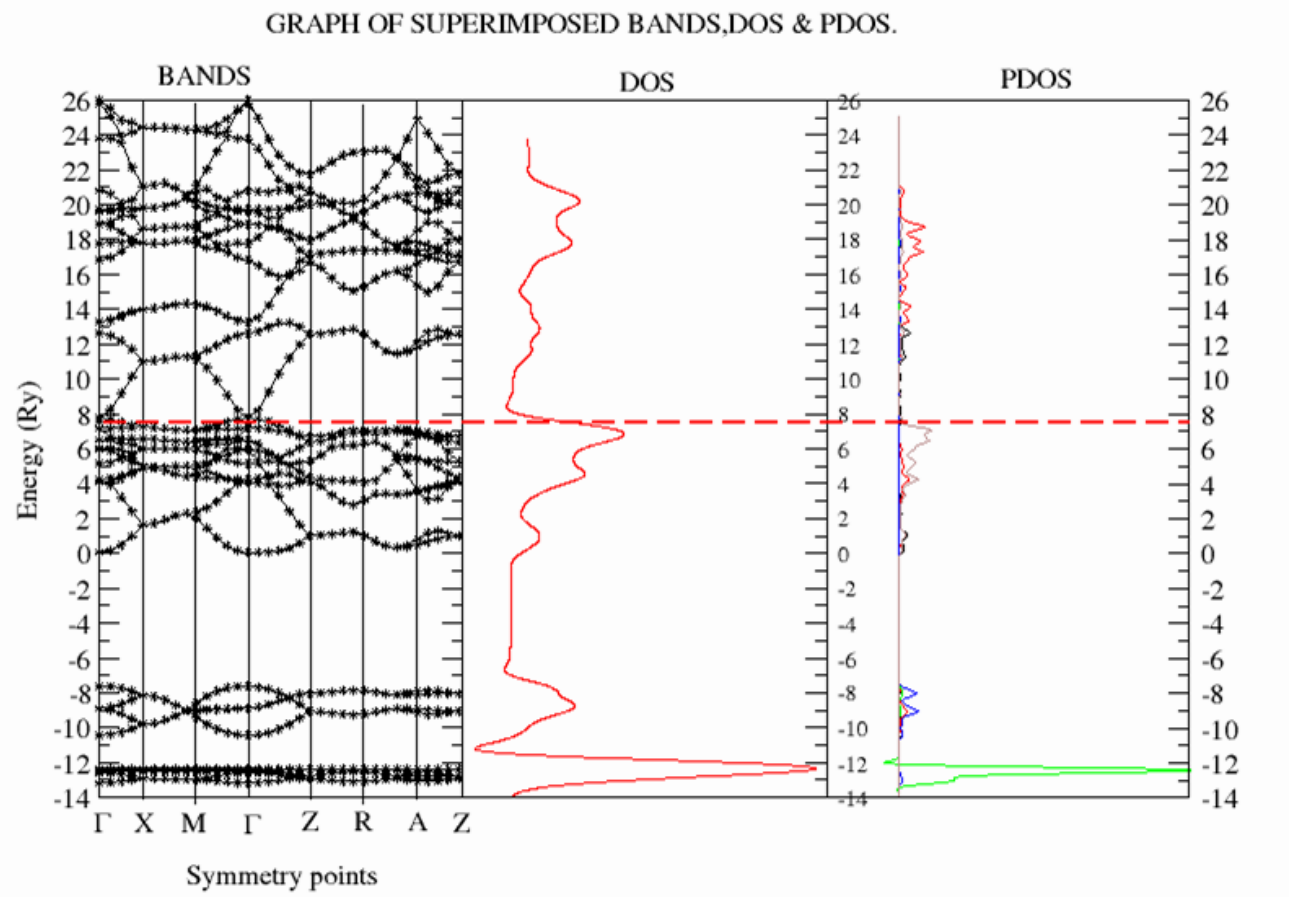

Fig.9b: graph of superimposed dos, pdos and bands.

5.4.0 OPTICAL PROPERTIES OF RUTILE TETRAGONAL SnO2 USING GW AND BSE.

DFT method cannot correctly predict the optical properties of SnO2. As such we seek other approaches such as Random Phase Approximation, Green function commonly known as electron propagator and dynamically screened interaction and the Bethe Salpeter Equation are used to investigate the optical properties of bc rutile tetragonal SnO2 structure.

The figure 10 shows the density of states of SnO2. As shown earlier by the DFT calculations, SnO2 exhibits continuous states. The graph of density of states below confirms this.

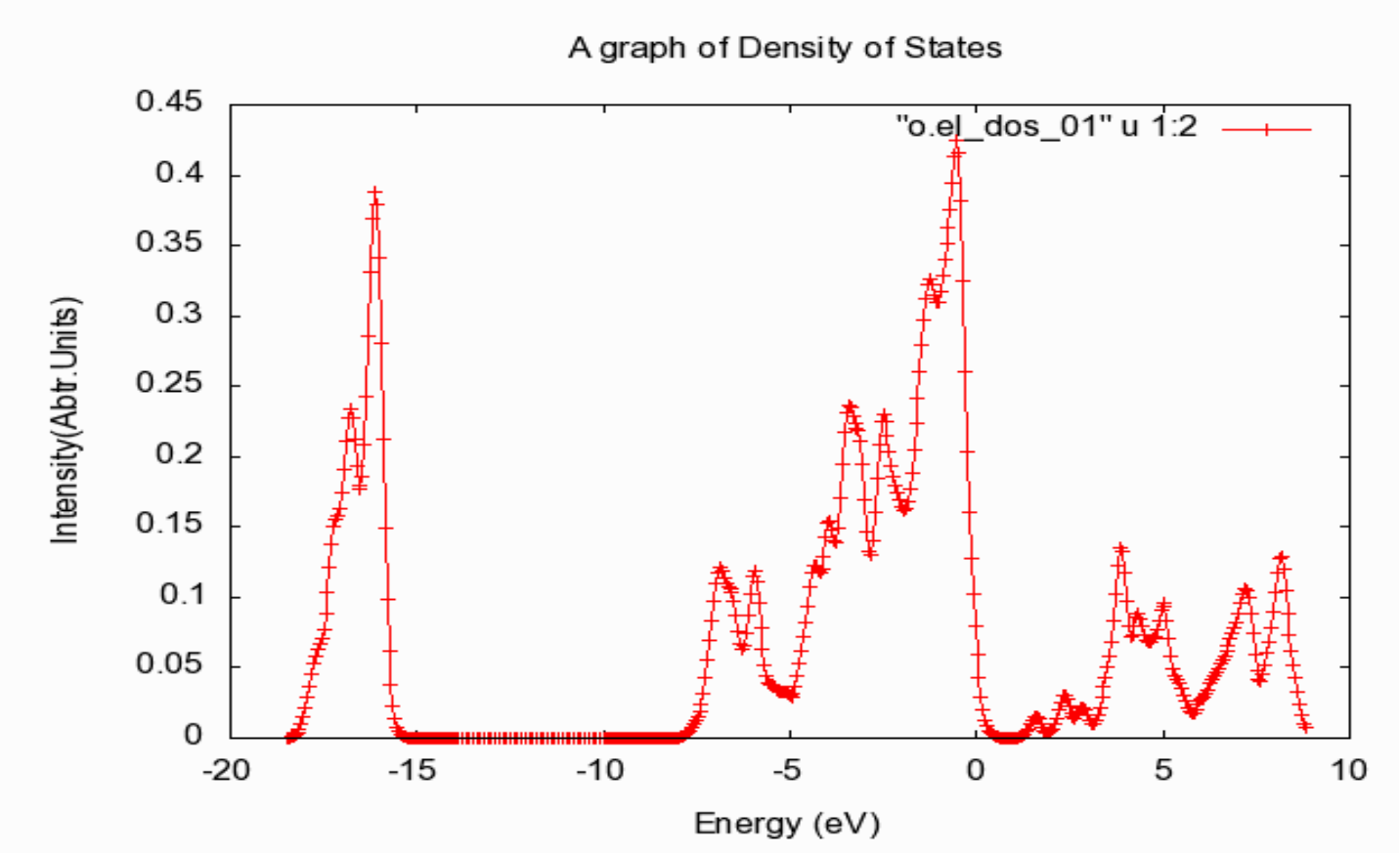

Fig.10.1: the graph of density of states.

The various graphs showing the optical properties for SnO2 were plotted and the results where as shown in the fig.10.2-4 below.

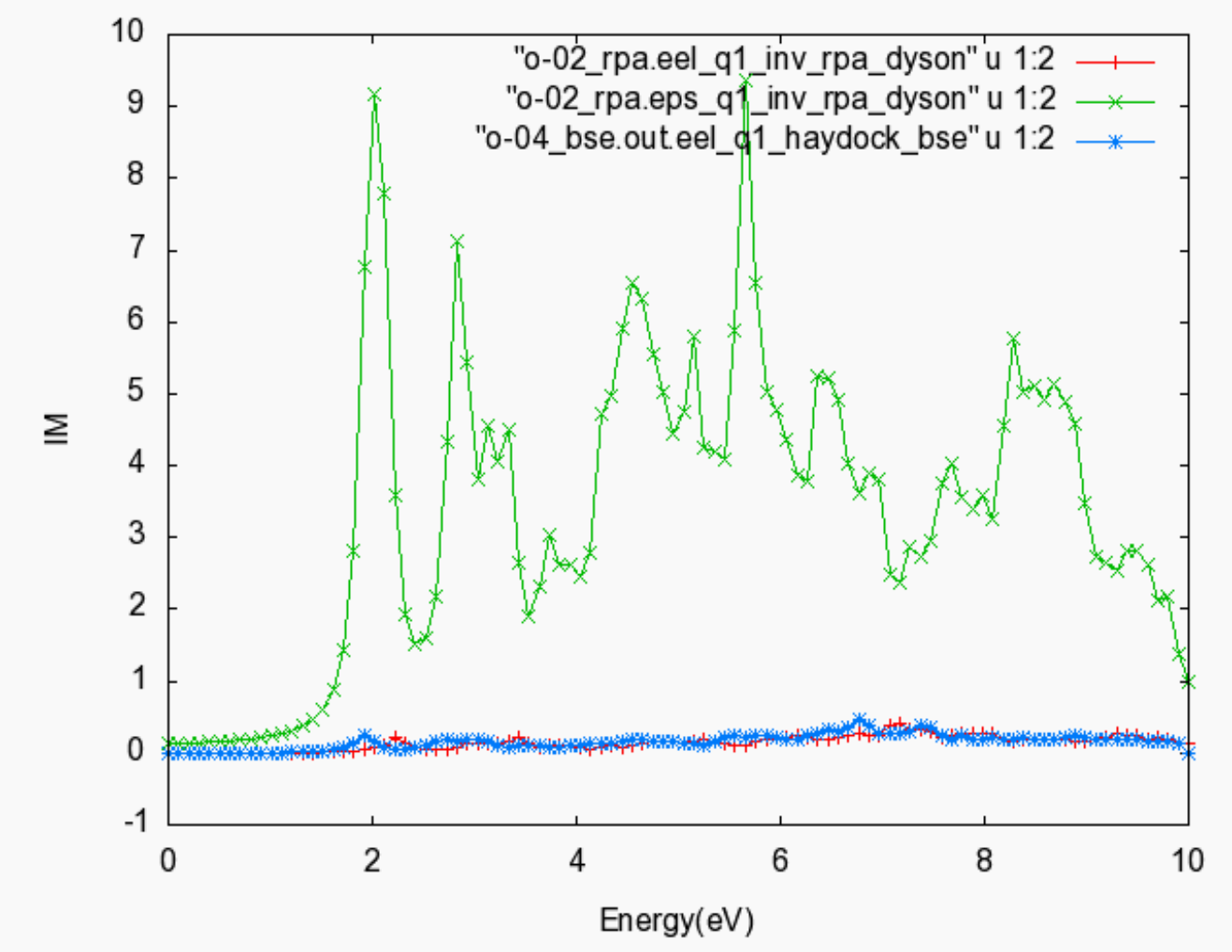

Fig10.2: the graph of energy against the GW-RPA and the BSE.

The first peaks were established at 2.0eV, 2.0eV and 2.34eV for the GW-RPA_EEL, GW-RPA_EPS and BSE methods respectively. The highest intensity peak of the absorption energy is realized GW-RPA (EPS) at 6.0eV, 6.84eV for BSE and the same is observed at 7.2eV for GW-RPA(eel). If we compare the BSE and the GW-RPA (EEL), it is evident that GW-RPA (EEL) has been shifted by 0.8eV to the left of BSE.

CONCLUSION.

DFT calculation predicts the rutile tetragonal SnO2 to be having an indirect band gap of 3.6eV a value that agrees with the existing experimental and theoretical results. The absorbency of SnO2 as predicted by the BSE equation is realized at a normal range which posses to the fact that tin oxide is good absorbent pointing to its good performance in a solar cell and other optoelectronic devices.

RECOMMENDATIONS.

For proper results to be realized on the rutile structure, one may need to consider using norm-conserving pseudo potentials as opposed to the ultra soft. Remember the choice of the pseudo potential to be used should consider the electronic configuration of the material and the valence occupancy of the pseudo potentials to be used.

Use of DFT+U calculation method would give better results than DFT calculation. Since SnO_2 is a good transparent conducting oxide, a study of the optical properties will increase the usability of this element. This can easily be done using the yambo coding system. In this case you need to note that you will have to use norm conserving pseudo potentials with much smaller values of k-points to save on the running time.

The electronic and optical properties take place on the surface of the material. I would therefore recommend that this study would have been more meaningful if would have been done on the surface of the material. I recommend surface analysis for this material to establish the best surfaces that can be used to realize best performance of SnO_2 as an optoelectronic material.

REFERRENCES.

[1] Matthias Batzill , Ulrike Diebold (2001). The surface and materials science of tin oxide, PP 3

[2]. M. Kwoka a, L. Ottaviano b , M. Passacantando b , G. Czempik a , S. Santucci b , J. Szuber a (2009) PP 467

[3]. S. Gubbala, a H. B. Russell, a H. Shah, b B. Deb, d J. Jasinski, d H. Rypkema c

and M. K. Sunkara a (2009) PP 145

[4]. M. Batzill, U. Diebold / Progress in Surface Science 79 (2005) 47–154

[5]. M. Radecka, J. Przewoznik, K. Zakrzewska, Thin Solid Films

391 (2001) PP 247.

[6]R. Kumar , I. Verma , N. Verma "Synthesis and Characterization of Tin Oxide as

Humidity Sensor" Department of Physics, University of Lucknow, Lucknow-226007, India

[7] V. Weener, H. Baur (1955) 'Uber die verfeinerung der Kristallstrukturbestimmung einiger vertreter des Rutiltyps:TiO2, SnO2, GeO2 and MgF2' PP 23

[8] C.Kelvin de Berg (2010) 'Tin Oxide chemistry from the last decade of the twenty – first century: Towarda the Development of a Big-Picture Approach to the Teaching and Learning of Chemistry while Focussing on aspecific compound or class of compounds.' PP 136

[9] Vandana Singh, C.K. Suman and Satyendra Kumar (2006) 'Indium Tin Oxide (ITO) films on flexible substrates for organic light emitting diodes' PP 456

[10]F.R. Sensato a,∗ , R. Custodio a , E. Longo , A. Beltrán c,∗ , J. Andrés c (2003) "Electronic and structural properties of Sn x Ti 1−x O 2 solid solutions: a periodic DFT study" PP 21

[11] Wilbur Johnson, Jr., M.S., (2013) 'Safety Assessment of Tin(IV) Oxide as Used in

Cosmetics report' PP 79

[12] Wilbur Johnson, Jr., M.S., (2012) 'Tin and Tin Oxide as Used in Cosmetics'PP53

[13] A. Marini, R. Del Sole, G. Onida, Phys. Rev. B 66 (2002) 115101; A. Marini, G. Onida, R. Del Sole, Phys. Rev. Lett. 88 (2002) 016403; A. Marini, G. Onida, R. Del Sole, Phys. Rev. B 64 (2001) 195125. PP 2

[14] H. Ehrenreich, The Optical Properties of Solids, Academic, New York, 1965. PP 57

[15] Z.W. Pan, Z.R. Dai, Z.L. Wang, Nanobelts of semiconducting oxides, Science 291 (2001) 1947. PP 5

[16] Z.R. Dai, Z.W. Pan, Z.L. Wang, Ultra-long single crystalline nanoribbons of tin oxide, Solid State Commun. 118 (2001) 351.

[17] Z.R. Dai, J.L. Gole, J.D. Stout, Z.L. Wang, Tin oxide nanowires, nanoribbons, and nanotubes, J. Phys. Chem. B 106 (2002) 1274.

[18] V.E. Heinrich, P.A. Cox, The Surface Science of Metal-oxides, Cambridge University Press, Cambridge, 1994. PP 43

[19] U. Diebold, The surface science of titanium dioxide, Surf. Sci. Rep. 48 (2003) PP 53.

[20] R.L. Hoffman, B.J. Norris, J.F. Wagner, ZnO-based transparent thin-film transistors, Appl. Phys. Lett. 82 (2003) PP 733.

[21] C.G. Granqvist, A. Hulta ker, Transparent and conducting ITO films: new developments and applications, Thin Solid Films 411 (2002) PP 1.

[22] K.L. Chopra, S. Major, D.K. Pandya, Transparent conductors—a status review, Thin Solid Films 102 (1983) PP 1.

[23] T.J. Coutts, D.L. Young, X. Li, Characterization of transparent conducting oxides, MRS Bull. 25 (2000) 58

[24] K. Ishiguro, T. Sasaki, T. Arai, I. Imai, Optical and electrical properties of tin oxide films, J. Phys. Soc. Jpn. 13 (1958) 296

[25] E.E. Kohnke, Electrical and optical properties of natural stannic oxide crystals, J. Phys.

Chem. Solids 23 (1962) 1557

[26] K. Suzuki, M. Mizuhashi, Structural, electrical and optical properties of r.f.-magnetron-sputtered SnO 2 :Sb film, Thin Solid Films 97 (1982) 119

[27] H.J. Herniman, D.R. Pyke, R. Reid, An investigation of the relationship between the bulk and surface composition of tin and antimony mixed oxide catalysts and the oxidative dehydrogenation of 1-butene to butadiene, J. Catal. 58 (1979) 68

[28] G.L.M.P Aponsu a , R.C.L de Silva b , and V.P.S Perera b, Vol. 9 (2008) 'Enhanced Photo voltaic effects of dye-sensitized solar cells of SnO 2 surface modified with gold nano particles' PP 675

[29] N.G. Park, M.G. Kang, K.S. Ryu, K.M. Kin, and S.H. Chang, J. Photochem. Photobiol. 161 (2004) PP 105.

[30] Giannozzi P., Baroni S. et. Al, (2009) 'QUANTUM ESPRESSO: a modular open-source software project for quantum simulations of materials," *Journal of physics: Condensed matter* Vol.21, No.39 PP 4

[31] Marini A., Hogan C., Gruning M., and Varsano D., (2009) "yambo: An ab initio tool for excited state calculations, "Computer Physics Communications, Vol. 180, No. 8 PP 213

[32] Salaneck, W.R.; L¨uglund, M.; Fahlmann, M.; Greczynski, G.; Kugler, T. The electronic structure of polymer-metal interfaces studied by ultraviolet photoelectron spectroscopy. *Mater. Sci. Eng. R*2001, *34*, 121–146.

[33] Rose, D.H.; Hasoon, F.S.; Dhere, R.G.; Albin, D.S.; Ribelin, R.M.; Li, X.S.; Mahathongdy, Y.; Gessert, T.A.; Sheldon, P. Fabrication procedures and process sensitivities for CdS/CdTe solar cells. *Prog. Photovolt. Res. Appl.* 1999, *7*, PP 331–340.

[34] Ferekides, C.S.; Mamazza, R.; Balasubramanian, U.; Morel, D.L. Transparent conductors and buffer layers for CdTe solar cells. *Thin Solid Films* 2005, PP *480–481*, 224–229.

[35] Harima, Y.; Yamashita, K.; Ishii, H. Energy structures of molecular semiconductors contacting metals under air studied by the diffusion potential measurements and the Kelvin probe technique. *Thin Solid Films* 2000, *366*, PP 237–248.

[36] D´Andrade, B.W.; Datta, S.; Forrest, S.R.; Djurovich, P.; Polikarpov, E.; Thompson, M.E.

Relationship between the ionization and oxidation potentials of molecular organic semiconductors. *Organic Electronics* 2005, *6*, PP 11–20.

[37] F.R. Sensato, R. Custódio, M. Calatayud, A. Beltrán, J. Andrés, J.R. Sambrano, E. Longo, Surf. Sci. 511 (2002) PP 408.

[38] M.W. Abee, D.F. Cox, Surf. Sci. 520 (2002) PP 65.

[39] V.R. Saunders, R. Dovesi, C. Roetti, M. Causà, N.M.Harrison, R. Orlando, C.M. Zicovich-Wilson, Crystal'98 User's Manual, University of Torino, Torino, 1998.PP 235

[40] A.D. Becke, J. Chem. Phys. 98 (1993) PP 5648.

[41] C. Lee, R.G. Yang, R.G. Parr, Phys. Rev. B 37 (1988) PP 785.

[42] C.-H. Hu, D.P. Chong, in: P. von Rague Schleyer (Ed.), Encyclopedia of Computational Chemistry, Wiley, Chichester, UK, 1998. PP 489

[43] J. Muscat, A. Wander, N.M. Harrison, Chem. Phys. Lett. 342 (2001) PP 397.

INPUT FILE FOR SnO2

```
&control
    restart_mode='from_scratch',
    calculation='scf',
    outdir = './',
    pseudo_dir='/home/masika/Applications/espresso-5.0.2/pseudo',
    prefix = 'Sn2O',
/
&SYSTEM
    ibrav=6,
    celldm(1)= 9.3,
    celldm(3)= 0.684,
    nat=  6, ntyp= 2,
    ecutwfc =100 ,
    ecutrho = 400,
    occupations='smearing',
    smearing='marzari-vanderbilt',
    degauss=0.05
/
&ELECTRONS
     mixing_mode = 'plain',
     mixing_beta = 0.7,
     conv_thr = 1.0e-8,
```

/

ATOMIC_SPECIES

Sn 50.011 Sn.pbe-hgh.UPF

O 15.9994 O.pbe-hgh.UPF

ATOMIC_POSITIONS {crystal}

Sn 0.000000000 0.000000000 0.000000000

Sn 0.500000000 0.500000000 0.500000000

O 0.313000000 0.313000000 0.000000000

O 0.813000000 0.187000000 0.500000000

O -0.313000000 -0.313000000 0.000000000

O -0.813000000 -0.187000000 0.500000000

K_POINTS automatic

6 6 9 0 0 0